Glycolysis-dependent Sulfur Metabolism Orchestrates Morphological Plasticity and Virulence in Fungi

Authors:

Dhrumi Shah[1,2], Adishree M[1], Nikita Rewatkar[1], Siddhi Gupta[1,2], Sudharsan Mathivathanan[1] and Sriram Varahan[1#]

Affiliations:

[1]CSIR-Centre for Cellular and Molecular Biology, Uppal Road, Hyderabad 500007, India.

[2]Academy of Scientific and Innovative Research (AcSIR), Ghaziabad- 201002, India.

#- Corresponding Author

Email: sriram@ccmb.res.in

Abstract

Fungi exhibit remarkable morphological plasticity, which allows them to undergo reversible transitions between distinct cellular states in response to changes in their environment. This phenomenon, termed fungal morphogenesis, is critical for fungi to survive and colonize diverse ecological niches and establish infections in a variety of hosts. Despite significant advancements in the field with respect to understanding the gene regulatory networks that control these transitions, the metabolic determinants of fungal morphogenesis remain poorly characterized. In this study, we uncover a previously uncharacterized, conserved dependency between central carbon metabolism and *de novo* biosynthesis of sulfur-containing amino acids that is critical for fungal morphogenesis, in two key fungal species. Using a multidisciplinary approach, we demonstrate that glycolytic flux is crucial to drive fungal morphogenesis and perturbation of this pathway leads to a significant downregulation in the expression of genes involved in *de novo* biosynthesis of sulfur-containing amino acids. Remarkably, exogenous supplementation of sulfur-containing amino acids (cysteine/methionine) or inorganic sulfate, robustly rescues the morphogenesis defect induced by the perturbation of glycolysis in both *Saccharomyces cerevisiae* and *Candida albicans*, underscoring the pivotal role of *de novo* biosynthesis of sulfur-containing amino acid as a downstream effector of morphogenesis. Furthermore, a *C. albicans* mutant lacking the glycolytic enzyme, phosphofructokinase (Pfk1) exhibited significantly reduced survival within *murine* macrophages and attenuated virulence in a *murine* model of systemic candidiasis. Overall, our research elucidates a previously uncharacterized coupling between glycolysis and sulfur metabolism that is critical for driving fungal morphogenesis, contributing to our understanding of this conserved phenomenon.

Key words: Fungal Morphogenesis, Glycolysis, *Saccharomyces cerevisiae, Candida albicans,* Virulence

Introduction

In response to changes in their environment, fungi exhibit remarkable morphological plasticity, allowing them to reversibly transition between specialized cell states. This inherent ability to rapidly adapt to the changes in their environment is essential for their survival and allows them to colonize diverse ecological niches including various host organisms [1–3]. This conserved phenomenon, of fungal morphogenesis, encompasses a plethora of morphological forms including pseudohyphae, hyphae and titan cells to name a few [1]. Importantly, these morphological transitions in various pathogenic fungal species significantly influence their interaction with the respective host, impacting their overall ability to cause persistent infections [4,5]. Fungal morphogenesis is conserved across a plethora of fungal species and has profound implications with respect to fungal ecology, anti-fungal resistance and pathogenicity across a spectrum of hosts [6–8]. Consequently, it has been a central focus of intense scientific investigation over the last several years [1,9]. While significant progress has been made in elucidating the intricate gene regulatory networks that govern these morphological transitions (e.g., Genetic networks that orchestrate yeast to pseudohyphal differentiation in *Saccharomyces cerevisiae* and yeast to hyphal differentiation in *Candida albicans* have been well characterized [10,11]), a critical knowledge gap persists regarding the underlying metabolic determinants of fungal morphogenesis. Despite the recognized influence of nutrient availability on fungal morphogenesis [12–14], our understanding of the specific metabolic networks and their regulatory influence on morphogenetic switching in fungi remain incompletely characterized.

In this study, we employed *Saccharomyces cerevisiae* and the human fungal pathogen, *Candida albicans* to dissect the metabolic underpinnings of fungal morphogenesis, under nitrogen-limiting conditions, a known trigger for morphogenetic switching in these fungi [15,16]. Our findings reveal a critical role for central carbon metabolism, particularly glycolysis, in facilitating the yeast-to-pseudohyphal transition in *S. cerevisiae* and the yeast-to-hyphal transition in *C. albicans*, both of which have been shown to be crucial for their survival and the ability of *C. albicans* to successfully infect a host [17,18]. Comparative transcriptomic analysis identified a conserved metabolic network crucial for these morphogenetic switching events under nitrogen-limiting conditions. Importantly, we observed that perturbations in glycolytic flux using pharmacological and genetic means, negatively impact the expression of genes involved in sulfur metabolism. Furthermore, our functional studies demonstrated that supplementation with sulfur-containing amino acids (cysteine or methionine) or inorganic sulfate, effectively rescued the morphogenetic defects resulting from glycolytic impairment, establishing a novel metabolic axis linking glycolysis and sulfur metabolism in the regulation of fungal morphogenesis. Finally, we investigated the implications of this glycolysis-dependent sulfur metabolism on the virulence of *C. albicans*. Our data demonstrates that a *C. albicans* mutant lacking genes that encode for a crucial glycolytic enzyme, phosphofructokinase, exhibits reduced survival within macrophages and severely attenuated virulence in an *in vivo murine* model of systemic candidiasis.

Collectively, our research, for the first time, identifies a previously uncharacterized metabolic axis linking glycolysis and sulfur metabolism under conditions that induce fungal morphogenesis and underscores the importance of this metabolic network in regulating fungal morphogenesis across two key fungal species and the ability of the human fungal pathogen, *C. albicans* to establish infection in a host. These findings address a fundamental

knowledge gap in the field and contributes significantly to our understanding of a broadly conserved phenomenon that exists across a plethora of fungal species.

Results

Quality and Quantity of Carbon Source Influences Fungal Morphogenesis

Nitrogen limitation is essential for yeast to pseudohyphae transition in *S. cerevisiae* [15,19]. However, the influence of carbon sources on this phenomenon is not completely understood. In order to determine whether the quality of carbon source influences fungal morphogenesis in *S. cerevisiae*, we tested the ability of fermentable carbon sources that contain glucose, such as sucrose, maltose and trehalose, as well as fermentable carbon sources that do not contain glucose but are metabolized *via* central carbon metabolic pathways [20], such as fructose, mannose and galactose, and non-fermentable carbon sources, such as ethanol, glycerol, acetate, and DL-glyceraldehyde, to induce pseudohyphal differentiation (Fig 1A and 1B). Nitrogen-limiting medium containing glucose was used as positive control as it has been shown to induce robust pseudohyphal differentiation [15,19,21]. Sucrose, maltose and trehalose were able to induce pseudohyphal differentiation similar to glucose, under nitrogen-limiting conditions (Fig 1A). Interestingly, all the non-glucose containing fermentable carbon sources including fructose, mannose and galactose were also able to induce pseudohyphal differentiation similar to glucose (Fig 1A). However, non-fermentable carbon sources including ethanol, glycerol, acetate, and DL-glyceraldehyde were unable to induce fungal morphogenesis under nitrogen-limiting conditions (Fig 1B). This demonstrates that the presence of fermentable carbon sources is critical for inducing fungal morphogenesis in *S. cerevisiae*, under nitrogen limitation. In order to determine if the presence of fermentable carbon sources is sufficient to induce pseudohyphal differentiation even in conditions that does not promote this phenomenon (in the presence of non-fermentable carbon sources), *S. cerevisiae* wild-type ∑1278b was spotted on nitrogen-limiting medium containing glucose and either one of the non-fermentable carbon sources. As shown in Fig 1C, presence of glucose is sufficient to induce fungal morphogenesis even in conditions that otherwise do not promote pseudohyphal differentiation. These results demonstrate that the presence of fermentable carbon sources *i.e*, glucose is required to induce pseudohyphal differentiation under nitrogen-limiting conditions.

We next asked if the quantity of carbon source influences fungal morphogenesis. To address this question, *S. cerevisiae* wild-type ∑1278b was spotted on nitrogen-limiting media (SLA) with varying glucose concentrations ranging from 0.1% to 4%. SLA medium containing 2% glucose was used as a positive control as this condition induces robust pseudohyphal differentiation (Fig 1A) and SLA medium containing 2% ethanol was used as a negative control, since this non-fermentable carbon sources fails to induce pseudohyphal differentiation (Fig 1B). Our data clearly demonstrates that glucose concentration positively influences pseudohyphal differentiation since nitrogen-limiting medium with 0.1% glucose exhibited significantly reduced pseudohyphal differentiation compared to nitrogen-limiting medium containing 2% glucose and nitrogen-limiting medium containing 4% glucose exhibited significantly increased pseudohyphal differentiation compared to nitrogen-limiting medium containing 2% (Fig 1D). We then isolated cells from these colonies and quantified the percentage of pseudohyphal cells

(cells with a length/width ratio of 2 or more [22]) in these colonies. SLA medium with 0.1% glucose had a significantly lower percentage of pseudohyphal cells compared to SLA medium with 2% glucose and SLA medium with 4% glucose had a significantly higher percentage of pseudohyphal cells compared to SLA medium with 2% glucose. As expected, SLA medium containing 2% ethanol had the least amount of pseudohyphal cells, overall (Fig 1D). Taken together, our results clearly demonstrate that glucose is a critical driver of fungal morphogenesis under nitrogen-limiting conditions.

Ability of Cells to Metabolize Glucose *via* Glycolysis is Critical for Fungal Morphogenesis

Our data clearly demonstrates that glucose is necessary for pseudohyphal differentiation under nitrogen-limiting conditions. Crabtree positive organisms like *S. cerevisiae* metabolize glucose primarily *via* glycolysis to meet their growth and energy demands (Fig 2A) [23,24]. In order to determine whether the ability of *S. cerevisiae* to metabolize glucose *via* glycolysis is critical for pseudohyphal differentiation under nitrogen-limiting conditions, we spotted *S. cerevisiae* wild-type ∑1278b on nitrogen-limiting media containing 2% glucose (SLAD) with and without sub-inhibitory concentrations of 2-Deoxy-D-Glucose (2DG) and sodium citrate (NaCi), which are well characterized glycolysis inhibitors [25,26] and monitored pseudohyphal differentiation. Our data demonstrates that sub-inhibitory concentrations of 2DG and NaCi significantly attenuated the ability of *S. cerevisiae* to undergo pseudohyphal differentiation (Fig 2B). We then isolated cells from these colonies and quantified the percentage of pseudohyphal cells (cells with a length/width ratio of 2 or more) in these colonies. Addition of 2DG or NaCi resulted in a significant reduction in pseudohyphal cells (Fig 2C) without compromising the overall growth of *S. cerevisiae* wild-type ∑1278b (Fig 2D). Another diploid *S. cerevisiae* strain that is known to undergo pseudohyphal differentiation under nitrogen-limiting conditions is the prototrophic CEN.PK strain [27]. In order to determine if our observations in ∑1278b can be recapitulated in CEN.PK, *S. cerevisiae* wild-type CEN.PK was spotted on SLAD with and without sub-inhibitory concentrations of 2-Deoxy-D-Glucose (2DG) and sodium citrate (NaCi). Our data clearly demonstrates that 2DG and NaCi strongly inhibit pseudohyphal differentiation (Fig 2B and 2C) without compromising the overall growth of *S. cerevisiae* wild-type CEN.PK as well (Fig 2D).

Given that, 2DG and NaCi exhibited a strong inhibitory effect on pseudohyphal differentiation under nitrogen-limiting conditions in a strain-independent manner, we wanted to corroborate these observations by using pertinent genetic knockout strains that are compromised in performing glycolysis, in the presence of glucose [28,29]. In order to do this, we generated knockout strains which lack the genes that encode for enzymes that are involved in the glycolysis pathway including *pfk1* (phosphofructokinase-1) and *adh1* (alcohol dehydrogenase-1) [30,31] (Fig 2E). Our result demonstrates that the deletion of *pfk1* and *adh1* in both the ∑1278b and CEN.PK backgrounds (*ΔΔpfk1* refers to the *pfk1* knockout strain and *ΔΔadh1* refers to the *adh1* knockout strain) resulted in a significant reduction in pseudohyphal differentiation, compared to the corresponding wild-type strains, under nitrogen-limiting conditions (Fig 2F). We then isolated cells from these colonies and quantified the percentage of pseudohyphal cells in these colonies. Deletion of *pfk1* and *adh1* resulted in a significant reduction in pseudohyphal cells (Fig 2G) corroborating our data obtained using the glycolytic inhibitors, 2DG and NaCi. In order to rule out whether the reduction in pseudohyphal differentiation in these mutants, is due to a general growth defect, we did spot dilution assays wherein serial dilutions of the wild-

type strains and pertinent knockout strains were spotted on SLAD (Fig 2H). Our data suggests that the reduction in pseudohyphal differentiation is not due to general growth defects as the mutants were able to grow similar to the wild-type strains in SLAD (Fig 2H). Taken together, our results clearly demonstrate that the ability of *S. cerevisiae* to efficiently metabolize glucose *via* glycolysis is critical for pseudohyphal differentiation under nitrogen-limiting conditions.

Comparative Transcriptomics Identifies Glycolysis-dependent Regulation of Sulfur Metabolism During Fungal Morphogenesis

Our previous data showed that the perturbation of glycolysis using specific inhibitors including 2DG/NaCi or deletion of genes that encode for glycolytic enzymes including *pfk1/ adh1* resulted in a significant reduction in pseudohyphal differentiation, under nitrogen-limiting conditions (Fig 2). Given that, glycolysis strongly influences the global transcriptional landscape of *S. cerevisiae* [32,33], we undertook a comprehensive transcriptomic approach to identify the changes in the transcriptional landscape of *S. cerevisiae* colonies, in conditions that perturb glycolysis, resulting in the inhibition of pseudohyphal differentiation. We performed comparative RNA-Seq analysis using RNA isolated from wild-type cells spotted on SLAD in the presence and absence of the glycolysis inhibitor, 2DG (2DG addition was used to perturb glycolysis in our transcriptomics experiments, as it exerted the strongest inhibitory effect on pseudohyphal differentiation as shown in Fig 2B and 2C). The experimental schematic is depicted in Fig 3A. Briefly, comparative RNA-Seq analysis was done using wild-type colonies grown on SLAD in the presence and absence of 2DG isolated on day 5 (D-5) and day 10 (D-10), respectively (Fig 3A). We have used D-5 as an early time point for our experiments, as we have consistently observed the emergence of pseudohyphae in colonies spotted on SLAD at this time-point and D-10 as a late time point wherein colonies exhibit robust pseudohyphal differentiation (S1A Fig). A volcano plot of differential gene expression in 2DG treated cells compared to untreated cells in both D-5 and D-10 is shown in Fig 3B wherein some of the significantly upregulated and downregulated genes are highlighted with blue colour. Previous studies in the field have shown that, under nitrogen-limiting/glucose-replete conditions, glycolytic intermediates provide various precursors needed for the biosynthesis of several amino acids in order to maintain amino acid homeostasis [34,35] and perturbation of glycolysis under these conditions results in the increased transcription of various genes involved in amino acid biosynthesis, as a feedback response (S1B Fig). As expected, the expression of many of the genes involved in amino acid biosynthesis and transport were significantly upregulated in 2DG treated cells compared to untreated cells, in both D-5 and D-10 respectively (S1C Fig) corroborating the observations from the previously mentioned studies [35,36]. Interestingly and rather unexpectedly, the expression of multiple genes specifically involved in the biosynthesis and transport of sulfur-containing amino acids, cysteine and methionine were significantly downregulated in 2DG treated cells compared to untreated cells in both D-5 and D-10 respectively (Fig 3C).

Our RNA-Seq analysis clearly demonstrates that multiple genes involved in the *de novo* biosynthesis of sulfur-containing amino acids, are significantly downregulated in the presence of 2DG, under nitrogen-limiting conditions. In order to determine whether these observed trends are reflected at the protein level, we generated strains wherein various proteins involved in the *de novo* biosynthesis of sulfur-containing amino acids including Met4p (Leucine-zipper transcriptional activator), Met32p (Zinc-finger DNA-binding transcription factor), Met16p (3'-phosphoadenylsulfate reductase), Met10p (Subunit alpha

of assimilatory sulfite reductase), Cys4p (Cystathionine beta-synthase) and Cys3p (Cystathionine gamma-lyase) were epitope-tagged (Fig 3D). These strains were spotted on SLAD in the presence and absence of 2DG following which, cells from colonies were isolated on D-5 and levels of these proteins were assessed by using western blotting (Fig 3E). Our results indicate that the levels of Met4p, Met32p, Met16p, Met10p, Cys4p and Cys3p were significantly reduced in the 2DG treated cells compared to untreated cells, corroborating our transcriptome data (Fig 3E & S2A Fig). This clearly demonstrates that perturbation of glycolysis negatively influences the expression of sulfur metabolism proteins, under nitrogen-limiting conditions. We next asked, if the glycolysis-dependent regulation of sulfur metabolism under nitrogen-limiting conditions (SLAD) is restricted to conditions wherein cells physically attach to solid surfaces (colony growth) or whether it is conserved even in conditions where cells are free-floating (liquid-culture growth). In order to do this, pertinent epitope-tagged strains (wherein Met32p, Met16p, Met10p and Cys3p were HA-tagged) were grown in liquid SLAD in the presence and absence of 2DG for 24 hours after which the expression of the aforesaid proteins were assessed using western blotting (S2B and S2C Fig). Importantly, our results indicate that the levels of Met32p, Met16p, Met10p and Cys3p were significantly reduced in the 2DG treated cells compared to untreated cells (S2B and S2C Fig). Taken together, our data clearly demonstrates that the perturbation of glycolysis under nitrogen-limiting conditions negatively influences sulfur metabolism.

Exogenous Supplementation of Sulfur Sources Rescues Fungal Morphogenesis Defects Caused by the Perturbation of Glycolysis

Our comparative transcriptomics data clearly demonstrates that, under nitrogen-limiting conditions, glycolysis plays a critical role in regulating the expression of genes involved in the *de novo* biosynthesis of sulfur-containing amino acids (Fig 3). Based on our previous data, we hypothesized that under nitrogen-limiting conditions, active glycolysis enables *de novo* biosynthesis of sulfur-containing amino acids which in turn, is critical for pseudohyphal differentiation and perturbation of active glycolysis using inhibitors like 2DG or disruption of genes involved in glycolysis including *pfk1* or *adh1* negatively affects glycolysis-mediated regulation of sulfur metabolism leading to attenuation of pseudohyphal differentiation (Fig 4A). If the proposed hypothesis holds true, the exogenous supplementation of sulfur-containing compounds should mitigate the fungal morphogenetic defects resulting from the perturbation of glycolysis. In order to test this, we performed sulfur add-back assays wherein *S. cerevisiae* wild-type ∑1278b was spotted on SLAD containing sub-inhibitory concentration of 2DG in the presence and absence of either sulfur-containing amino acids (cysteine or methionine) or an inorganic sulfur source like sodium sulfate which is metabolized *via* the sulfur assimilation pathway to synthesize cysteine and methionine (Fig 3D). Remarkably, the exogenous addition of cysteine resulted in a significant rescue of the pseudohyphal differentiation defect observed in nitrogen-limiting medium containing 2DG (Fig 4B). Corroborating this observation, the percentage of pseudohyphal cells in colonies isolated from SLAD containing 2DG and cysteine were significantly higher than the percentage of pseudohyphal cells in colonies isolated from SLAD containing 2DG alone (Fig 4C), Interestingly, the addition of methionine or sodium sulfate failed to rescue the pseudohyphal differentiation defects caused by the perturbation of glycolysis (Fig 4B and 4C).

We next asked if the exogenous addition of sulfur sources rescues the pseudohyphal differentiation defect exhibited by glycolysis defective strains, *ΔΔpfk1* and *ΔΔadh1*. In

order to do this, we performed similar sulfur add-back assays wherein *S. cerevisiae* wild-type ∑1278b along with *ΔΔpfk1* and *ΔΔadh1* strains were spotted on SLAD in the presence and absence of either sulfur-containing amino acids (cysteine or methionine) or sodium sulfate. Remarkably, the exogenous addition of either of these sulfur sources (cysteine or methionine or sodium sulfate) was able to completely rescue the pseudohyphal differentiation defect exhibited by the *ΔΔpfk1* and *ΔΔadh1* strains (Fig 4D). Corroborating this observation, the percentage of pseudohyphal cells in *ΔΔpfk1* and *ΔΔadh1* colonies isolated from SLAD containing cysteine or methionine or sodium sulfate were significantly higher than the percentage of pseudohyphal cells in *ΔΔpfk1* and *ΔΔadh1* colonies isolated from SLAD alone (Fig 4E). Taken together, our results clearly demonstrate that the glycolysis-mediated regulation of sulfur metabolism is critical for pseudohyphal differentiation under nitrogen-limiting conditions.

Sulfur Metabolism is Critical for Fungal Morphogenesis Under Nitrogen-limiting Conditions

Our previous observations strongly suggest a direct role for sulfur metabolism in regulating fungal morphogenesis, under nitrogen-limiting conditions. In order to determine whether glycolysis-dependent sulfur metabolism is critical for pseudohyphal differentiation, under nitrogen-limiting conditions, we generated pertinent knockout strains wherein various genes that are involved in the *de novo* biosynthesis of sulfur-containing amino acids were deleted *via* homologous recombination and we tested the ability of these deletion strains to undergo pseudohyphal differentiation, under nitrogen-limiting conditions. Briefly, we generated strains which lack genes involved in the *de novo* biosynthesis of sulfur-containing amino acids including *met32* (Zinc-finger DNA-binding transcription factor), *met3* (ATP sulfurylase), *met16* (3'-phosphoadenylsulfate reductase), *met5* (Sulfite reductase beta subunit), *met10* (Subunit alpha of assimilatory sulfite reductase), *met17* (O-acetyl homoserine-O-acetyl serine sulfhydrylase), *met2* (L-homoserine-O-acetyltransferase) and *met13* (Major isozyme of methylenetetrahydrofolate reductase) (Fig 3D). Deletion of *met32* and *met3* resulted in a significant reduction in pseudohyphal differentiation. Corroborating this observation, the percentage of pseudohyphal cells in *ΔΔmet32* and *ΔΔmet3* colonies were significantly lower in SLAD, compared to *S. cerevisiae* wild-type ∑1278b colonies (Fig 4F). This suggests that perturbations to sulfur metabolism negatively affects pseudohyphal differentiation. We next tested the ability of *ΔΔmet16, ΔΔmet5, ΔΔmet10, ΔΔmet17, ΔΔmet2* and *ΔΔmet13* strains to undergo pseudohyphal differentiation under nitrogen-limiting conditions. All the strains exhibited substantial defects in their ability to undergo pseudohyphal differentiation and the percentage of pseudohyphal cells were significantly lower in the colonies of all these strains compared to *S. cerevisiae* wild-type ∑1278b colonies (Fig 4G). Notably, *ΔΔmet5, ΔΔmet10, ΔΔmet17, ΔΔmet2* and *ΔΔmet13* strains also exhibited a growth defect in SLAD consistent with what has been reported in the literature [37].

Given that the aforesaid deletion strains are compromised in their ability to synthesize sulfur-containing amino acids [38,39], we wanted to confirm whether the pseudohyphal differentiation defects exhibited by these strains are solely due to this. In order to do this, we performed a simple sulfur add-back assay, wherein *ΔΔmet32*, *ΔΔmet3*, *ΔΔmet16*, *ΔΔmet5*, *ΔΔmet10*, *ΔΔmet17*, *ΔΔmet2* and *ΔΔmet13* strains were spotted on SLAD containing either cysteine, methionine or inorganic sulfur source like sodium sulfate and allowed to undergo pseudohyphal differentiation. Our results show that the addition of cysteine, methionine or sodium sulfate completely rescued the pseudohyphal

379 differentiation defect exhibited by *ΔΔmet32* strain. The percentage of pseudohyphal cells
380 were also significantly higher in *ΔΔmet32* colonies growing on SLAD containing cysteine,
381 methionine or sodium sulfate compared to just SLAD (Fig 4H). Expectedly, only cysteine
382 and methionine add-back resulted in the complete rescue of pseudohyphal differentiation
383 defect exhibited by *ΔΔmet3*, *ΔΔmet16*, *ΔΔmet5*, *ΔΔmet10* and *ΔΔmet17* strains and the
384 percentage of pseudohyphal cells were also significantly higher in *ΔΔmet3*, *ΔΔmet16*,
385 *ΔΔmet5*, *ΔΔmet10* and *ΔΔmet17* colonies growing on SLAD containing cysteine and
386 methionine compared to just SLAD alone. Sodium sulfate was unable to rescue the
387 pseudohyphal differentiation defect exhibited by these strains, as Met3p, Met16p, Met5p,
388 Met10p and Met17p are known to be sequentially involved in the incorporation of inorganic
389 sulfur into the biosynthesis of cysteine and methionine (Met3p catalyses the activation of
390 inorganic sulfate in an ATP-dependent reaction and forms the products, adenosine-5'-
391 phosphosulfate (APS) and pyrophosphate (PPi). Met16p reduces 3'-phosphoadenylyl
392 sulfate to adenosine-3',5'-bisphosphate and releases free sulfite. Met5p and Met10p are
393 part of sulfite reductase complex which converts sulfite into sulfate and Met17p catalyses
394 the reaction between O-acetyl-L-homoserine with a thiol to produce homocysteine [37])
395 (Fig 4H). Finally, only methionine add-back resulted in the complete rescue of
396 pseudohyphal differentiation defect exhibited by *ΔΔmet2* and *ΔΔmet13* including a
397 significant increase in the percentage of pseudohyphal cells (Fig 4H), as Met2p (encodes
398 for homoserine O-acetyltransferase) and Met13p (encodes for methylenetetrahydrofolate
399 reductase) have been shown to be essential for the synthesis of methionine from cysteine
400 and inorganic sulfur sources [40,41]. Taken together, our data clearly demonstrates that
401 the efficient *de novo* biosynthesis of sulfur-containing amino acids including cysteine and
402 methionine is critical for pseudohyphal differentiation, under nitrogen-limiting conditions.
403
404 **Glycolysis-dependent Sulfur Metabolism is Critical for Fungal Morphogenesis in**
405 ***Candida albicans***
406
407 *C. albicans* is an opportunistic fungal pathogen that exhibits a remarkable degree of fungal
408 morphogenesis in response to various environmental cues [42]. Yeast to hyphal
409 differentiation in *C. albicans* is well studied. However, we do not have a complete
410 understanding of fundamental metabolic drivers that orchestrate this phenomenon. Given
411 that central carbon metabolic pathways including glycolysis are well conserved across a
412 plethora of fungal species including *C. albicans* [43] and nitrogen limitation is one of the
413 key triggers for yeast to hyphal differentiation in *C. albicans* [16], we wanted to determine
414 if glycolysis-mediated sulfur metabolism plays an important role in this morphogenetic
415 switching in *C. albicans* as well. First, we wanted to determine if glycolysis is essential for
416 regulating fungal morphogenesis in *C. albicans*, under nitrogen-limiting conditions. In
417 order to do this, *C. albicans* wild-type SC5314 was spotted on nitrogen-limiting medium
418 (SLA) containing either glucose or non-fermentable carbon sources including ethanol or
419 glycerol, and allowed to grow for 7 days at 37 °C. Cells were isolated from these colonies
420 and imaged using bright-field microscopy. Our data clearly shows that in the presence of
421 glucose, *C. albicans* exhibits robust hyphal differentiation under nitrogen-limiting
422 conditions while hyphal differentiation was significantly reduced in SLA containing non-
423 fermentable carbon sources including ethanol and glycerol (Fig 5A). We then isolated cells
424 from these colonies and quantified the percentage of hyphal cells (cells with a length/width
425 ratio of 4.5 or more [44]) in these colonies. Corroborating our microscopy data, the
426 percentage of hyphal cells in nitrogen-limiting medium containing ethanol or glycerol was
427 significantly lower compared to the percentage of hyphal cells in nitrogen-limiting medium
428 containing glucose (Fig 5A). This data suggests that the presence of glucose is critical for

429 fungal morphogenesis in *C. albicans*. We next wanted to understand whether the ability of
430 C. *albicans* cells to metabolize glucose, under nitrogen-limiting conditions is critical for
431 fungal morphogenesis. In order to do this, *C. albicans* wild-type SC5314 was spotted on
432 SLAD, in the presence and absence of sub-inhibitory concentration of glycolysis inhibitor,
433 2DG, allowed to grow for 7 days, and cells were isolated and imaged using bright-field
434 microscopy. Our data clearly demonstrates that sub-inhibitory concentration of 2DG
435 significantly reduced filamentation in *C. albicans* (Fig 5B). We then isolated cells from
436 these colonies and quantified the percentage of hyphal cells in these colonies.
437 Corroborating our microscopy data, the percentage of hyphal cells in colonies spotted on
438 SLAD containing 2DG was significantly lower compared to the percentage of hyphal cells
439 in colonies spotted on SLAD without 2DG (Fig 5B). Taken together, our results show that
440 the ability of *C. albicans* to metabolize glucose is critical for fungal morphogenesis.
441
442 Given that the perturbation of glycolysis under nitrogen-limiting conditions, using 2DG
443 exhibited a strong inhibitory effect on hyphal differentiation in *C. albicans* (Fig 5B), similar
444 to what we observed in *S. cerevisiae*, we wanted to determine if the expression of genes
445 involved in the *de novo* biosynthesis of sulfur-containing amino acids are affected when
446 glycolysis is perturbed in *C. albicans*, under nitrogen-limiting conditions (similar to what
447 we observed in *S. cerevisiae*) [45]. In order to determine this, we spotted *C. albicans*
448 wild-type SC5314 on SLAD, in the presence and absence of 2DG and cells from colonies
449 were isolated after ~4 days (time point at which, we start to see robust hyphal
450 differentiation in *C. albicans* (S3A Fig)) for RNA isolation. We then performed comparative
451 RT-qPCR to check for the relative expression of genes involved in *de novo* biosynthesis of
452 sulfur-containing amino acids including *met32* (DNA-binding transcription factor), *met3*
453 (ATP sulfurylase), *met14* (Adenylylsulfate kinase), *met16* (3'-phosphoadenylsulfate
454 reductase), *met5* (*ecm17*) (Sulfite reductase beta subunit), *met10* (Sulfite reductase),
455 *met17* (*met15*) (O-acetyl homoserine-O-acetyl serine sulfhydrylase) and *cys3*
456 (Cystathionine gamma-lyase) [45–47], in cells isolated from colonies grown on SLAD
457 containing 2DG compared to cells isolated from colonies grown on SLAD without 2DG (Fig
458 5C). Our data clearly shows that all the aforesaid genes involved in *de novo* biosynthesis
459 of sulfur-containing amino acids pathway including *met32*, *met3*, *met14*, *met16*, *met5*,
460 *met10*, *met17* and *cys3* were significantly downregulated in the presence of 2DG (Fig 5D)
461 suggesting that perturbation of glycolysis negatively impacts sulfur metabolism in *C.*
462 *albicans*, under nitrogen-limiting conditions.
463
464 To determine if the significant reduction in hyphal differentiation that we observed in the
465 presence of 2DG can be attributed to the reduced expression of genes involved in the
466 *de novo* biosynthesis of sulfur-containing amino acids, we performed sulfur add-back
467 assays similar to what was done in *S. cerevisiae* (Fig 4B), wherein *C. albicans* wild-type
468 SC5314 was spotted on SLAD containing 2DG in the presence and absence of cysteine and
469 methionine (Fig 5E), allowed to grow for 7 days, and cells were isolated and imaged using
470 bright-field microscopy. Remarkably, the presence of cysteine and methionine significantly
471 rescued hyphal differentiation defects in the presence of 2DG (Fig 5F and 5G). We then
472 isolated cells from these colonies and quantified the percentage of hyphal cells.
473 Corroborating our microscopy data, the percentage of hyphal cells in colonies spotted on
474 SLAD containing 2DG with cysteine or methionine were significantly higher compared to
475 the percentage of hyphal cells in colonies spotted on SLAD with 2DG alone (Fig 5F and
476 5G). Overall, our data suggests that glycolysis-mediated regulation of sulfur metabolism
477 is critical for hyphal differentiation of *C. albicans*, under nitrogen-limiting conditions

478 highlighting the remarkable similarities with respect to the regulation of fungal
479 morphogenesis, between *S. cerevisiae* and *C. albicans*.
480
481 **Perturbation of Glycolysis Leads to Attenuated Fungal Virulence**
482
483 Our previous results clearly demonstrate that glycolysis and glycolysis-dependent sulfur
484 metabolism is critical for fungal morphogenesis of *C. albicans*, under nitrogen-limiting
485 conditions. In order to corroborate these observations by using pertinent genetic knockout
486 strains that are compromised in performing glycolysis, we generated a double knockout
487 strain lacking the gene that encodes for the glycolytic enzyme, phosphofructokinase (Pfk1)
488 using the SAT-Flipper method [48]. We then tested the ability of this deletion strain to
489 undergo hyphal differentiation under nitrogen-limiting conditions. Briefly, *C. albicans* wild-
490 type SC5314 and *ΔΔpfk1* were spotted on SLAD, allowed to grow for 7 days, and cells
491 were isolated and imaged using bright-field microscopy. Our result shows that the *ΔΔpfk1*
492 strain exhibits a significant reduction in hyphal differentiation compared to *C. albicans*
493 wild-type SC5314, under nitrogen-limiting conditions (Fig 6A). We then isolated cells from
494 these colonies and quantified the percentage of hyphal cells in these colonies.
495 Corroborating our microscopy data, the percentage of hyphal cells in *C. albicans* wild-type
496 SC5314 colonies spotted on SLAD were significantly higher compared to the percentage
497 of hyphal cells in *ΔΔpfk1* colonies (Fig 6A). Our previous results showed that the
498 perturbation of glycolysis in *C. albicans*, under nitrogen-limiting conditions, negatively
499 influences sulfur metabolism and this in turn might be causal for the reduced hyphal
500 differentiation observed in these conditions since the add-back of sulfur-containing amino
501 acids completely reverses this phenotype (Fig 5F and 5G). Given this, we wanted to
502 determine if the hyphal differentiation defect exhibited by *ΔΔpfk1* can be rescued by the
503 addition of sulfur-containing amino acids. In order to do this, we performed sulfur add-
504 back assays wherein *ΔΔpfk1* strain was spotted on SLAD in the presence and absence of
505 cysteine and methionine and allowed to grow for 7 days at 37 °C and imaged using bright
506 field microscopy. Interestingly, our data shows that only cysteine was able rescue the
507 hyphal differentiation defect exhibited by the *ΔΔpfk1* strain (Fig 6B). We then isolated cells
508 from these colonies and quantified the percentage of hyphal cells. Corroborating our
509 microscopy data, the percentage of hyphal cells in *ΔΔpfk1* colonies spotted on SLAD
510 containing cysteine were significantly higher compared to the percentage of hyphal cells
511 in *ΔΔpfk1* colonies spotted on SLAD alone (Fig 6B). Taken together, our results
512 demonstrate that the genetic perturbation of glycolysis *via* the deletion of the *pfk1* gene
513 significantly attenuates fungal morphogenesis under nitrogen-limiting condition and this
514 can be fully rescued by the addition of sulfur-containing amino acid, cysteine, reiterating
515 the importance of glycolysis-mediated regulation of sulfur metabolism in orchestrating
516 fungal morphogenesis in *C. albicans*.
517
518 Several studies have established the importance of fungal morphogenesis as a key
519 virulence strategy used by *C. albicans* to establish successful infections in the host [49–
520 51]. Given that *ΔΔpfk1*, displayed a significant attenuation in its ability to undergo hyphal
521 differentiation, we wanted to determine if this deletion strain was compromised in its ability
522 to infect the host. In order to do this, we took a two-pronged approach wherein, we first
523 tested the ability of the *ΔΔpfk1* strain to survive the harsh intracellular environment of the
524 macrophages which *C. albicans* encounters during various stages of host infection [52–
525 54]. We performed an *ex vivo* microbial survival assay wherein *RAW 264.7* macrophages
526 were incubated either with *C. albicans* wild-type SC5314 or the *ΔΔpfk1* strain for one hour
527 following which macrophages were lysed and fungi were serially diluted and plated to

528 determine the viable population of the *C. albicans* wild-type SC5314 and the *ΔΔpfk1* strain
529 (Fig 6C). We also calculated the percentage of the wild-type or mutant strain that survived
530 the incubation with the macrophages. Our results demonstrate that the viable population
531 of *ΔΔpfk1* strain was significantly lower compared to the wild-type strain, after incubation
532 with the macrophages (Fig 6C). Similarly, the percentage survival of the *ΔΔpfk1* strain
533 was significantly lower than the wild-type strain as well (Fig 6C). Overall, this data
534 indicates that the *ΔΔpfk1* strain is compromised with respect to macrophage survival.
535
536 Given that the *ΔΔpfk1* strain was significantly attenuated in the macrophage survival
537 assay, we next wanted to test the ability of this deletion strain to establish systemic
538 infection in a host. In order to do this, we challenged healthy wild-type C57BL/6 mice
539 intravenously with a dose of 10^7 CFU/ml (lethal dose [55]) of *C. albicans* wild-type SC5314
540 or *ΔΔpfk1* strain *via* lateral tail vein injection. This is an established *murine* model of
541 systemic candidiasis in the field and faithfully mimics the infection that occurs in humans
542 [56]. We then monitored survival of the infected animals for 21 days. Mice challenged with
543 *ΔΔpfk1* strain had significantly increased survival compared to mice challenged with
544 *C. albicans* wild-type SC5314 (Fig 6D). *C. albicans* exhibits strong tropism towards kidneys
545 during *murine* infections [57,58] and in order to measure the fungal burden within the
546 host, kidneys from C57BL/6 mice infected with both *C. albicans* wild-type SC5314 and
547 *ΔΔpfk1* were harvested ~2 days post infection (when the mice injected with wild-type
548 *C. albicans* SC5314 becomes moribund), homogenized and plated to measure the fungal
549 burden by enumerating the colony forming units (CFU) (Fig 6E). Our data indicates that
550 kidneys isolated from mice challenged with the *ΔΔpfk1* strain had significantly lesser CFU
551 compared to kidneys isolated from mice challenged with the *C. albicans* wild-type SC5314
552 (Fig 6F). We also performed histological analysis on the infected kidneys using GMS
553 staining (Grocott Methenamine Silver staining), to visualize the fungi (stained black) in
554 the tissue. Kidneys isolated from mice challenged with the *C. albicans* wild-type SC5314
555 had higher amounts of fungi compared to kidneys isolated from mice challenged with the
556 *ΔΔpfk1* strain (Fig 6G). Overall, our data indicates that the perturbation of glycolysis
557 significantly attenuates *C. albicans* virulence.
558

559 **Discussion**

560
561 Our findings provide compelling evidence for a conserved metabolic network that
562 intricately links central carbon metabolism (particularly glycolysis), sulfur amino acid
563 biosynthesis, and fungal morphogenesis in both *Saccharomyces cerevisiae* and *Candida*
564 *albicans*. We demonstrate that while nitrogen starvation is a known prerequisite [15,16]
565 for fungal morphogenesis, the availability of a fermentable carbon source, specifically
566 glucose, is equally essential for the yeast-to-pseudohyphae/hyphal transitions. Initially,
567 we established that the quality and quantity of glucose profoundly influence pseudohyphal
568 differentiation in *S. cerevisiae* under nitrogen-limiting conditions. Specifically, fermentable
569 carbon sources, irrespective of whether they contain glucose (sucrose, maltose, trehalose)
570 or not (fructose, mannose, galactose), robustly induce fungal morphogenesis, while non-
571 fermentable carbon sources (ethanol, acetate, glycerol, DL-glyceraldehyde) are unable to
572 do so in spite of their ability to support the regular growth of *S. cerevisiae* [59,60],
573 highlighting the critical requirement for fermentable carbon sources in this process.
574 Additionally, the presence of glucose, was sufficient to induce pseudohyphal differentiation
575 even in the presence of non-fermentable carbon sources, demonstrating its sufficiency in

576 triggering fungal morphogenesis. We also demonstrated a clear positive correlation
577 between glucose concentration and the extent of pseudohyphal differentiation, with both
578 colony morphology and quantification of pseudohyphal cells showing a dose-dependent
579 response. This emphasizes the quantitative importance of glucose availability in driving
580 fungal morphogenesis in *S. cerevisiae*. Glucose in the extracellular environment can be
581 sensed by *S. cerevisiae* using multiple proteins. One such protein is the well characterized
582 G-protein couple receptor (GPCR), Gpr1p. Binding of glucose to Gpr1p activates a
583 downstream signalling cascade, resulting in the production of cAMP which activates Protein
584 Kinase A (PKA) [61,62]. This glucose-dependent cAMP-PKA pathway has been shown to
585 be essential for pseudohyphal differentiation under nitrogen-limiting conditions [63].
586 However, the role of glucose as a metabolite in the context of pseudohyphal differentiation
587 is not known. Building upon our data that fermentable carbon sources (glucose containing
588 and non-glucose containing) that are metabolized *via* glycolysis are able to robustly induce
589 fungal morphogenesis, we next asked whether the ability of these cells to undergo active
590 glycolysis is critical for fungal morphogenesis. We took a two-pronged approach which
591 involved pharmacological or genetic perturbation of glycolysis, to address this question.
592 Perturbation of glycolysis using sub-inhibitory concentrations of well-characterized
593 inhibitors [25,26], 2DG or sodium citrate (NaCi) significantly attenuated pseudohyphal
594 differentiation in both *S. cerevisiae* strains (∑1278b and CEN.PK) that are known to
595 undergo pseudohyphal differentiation, without compromising overall growth. This strain-
596 independent effect was further corroborated by genetic evidence wherein deletion of key
597 glycolytic enzyme-encoding genes, *pfk1* and *adh1*, in both the strain backgrounds
598 (∑1278b and CEN.PK) also resulted in a significant reduction in pseudohyphal
599 differentiation, without causing general growth defects. These convergent findings strongly
600 support the notion that active glycolytic is essential for fungal morphogenesis under
601 nitrogen-limiting conditions.
602
603 To gain deeper insights underlying the glycolysis-mediated regulation of fungal
604 morphogenesis, we performed comparative transcriptomics on *S. cerevisiae* wild-type
605 cells grown under nitrogen-limiting conditions with and without the glycolysis inhibitor 2DG
606 (which had the strongest inhibitory effect on pseudohyphal differentiation). As anticipated,
607 genes involved in amino acid biosynthesis and transport were upregulated in the 2DG
608 treated cells, consistent with a feedback response that cells exhibits when glycolysis is
609 perturbed under nitrogen-limiting conditions, as various intermediates of glycolysis are
610 known to serve as precursors for the biosynthesis of several amino acids under these
611 conditions [34,35]. Remarkably, we observed a striking and unexpected downregulation
612 of multiple genes specifically involved in the biosynthesis and transport of sulfur-containing
613 amino acids, cysteine and methionine, in the 2DG treated cells at both early and late time
614 points of pseudohyphal development. This transcriptional downregulation was further
615 validated at the protein level for key proteins involved in the sulfur assimilation pathway
616 (Met4p, Met32p, Met16p, Met10p, Cys4p and Cys3p), clearly demonstrating the
617 dependence of sulfur metabolism on active glycolysis during fungal morphogenesis. This
618 unexpected link between central carbon metabolism and sulfur metabolism is not
619 restricted to conditions that induce fungal morphogenesis *i.e.* in surface-attached colonies
620 grown in nitrogen-limiting conditions since even in liquid cultures that have limiting levels
621 of nitrogen, wherein *S. cerevisiae* cells do not undergo pseudohyphal differentiation [64],
622 perturbation of glycolysis with 2DG results in significantly reduced expression of proteins
623 involved in the sulfur assimilation pathway (Met32p, Met16p, Met10p and Cys3p).
624

625 Given that multiple genes that encode for proteins involved in *de novo* biosynthesis of
626 sulfur-containing amino acids were downregulated in the presence of 2DG, which strongly
627 inhibits fungal morphogenesis, we wanted to explore the possibility that perturbation of
628 sulfur metabolism is causal for the attenuation of fungal morphogenesis in the presence
629 of 2DG. We tested the functional relevance of this glycolysis-dependent regulation of sulfur
630 metabolism in fungal morphogenesis directly through exogenous supplementation of
631 sulfur sources. The functional significance of glycolysis-dependent regulation of sulfur
632 metabolism was demonstrated through our sulfur add-back experiments wherein,
633 exogenous supplementation with cysteine specifically rescued the pseudohyphal
634 differentiation defect exhibited by *S. cerevisiae* in the presence of 2DG. Interestingly,
635 methionine alone was unable to rescue the pseudohyphal differentiation defect, in the
636 presence of 2DG even at various different concentrations (50μM, 100 μM, 200μM and
637 500μM). Expectedly, addition of inorganic sulfate was unable to rescue the 2DG induced
638 pseudohyphal differentiation defect since multiple genes that encode for the proteins
639 involved in the sulfur assimilation pathway (Met3, Met5, Met10 and Met16), were
640 significantly downregulated in the presence of 2DG. Furthermore, the pseudohyphal
641 differentiation defects observed in the *ΔΔpfk1* and *ΔΔadh1* strains were completely
642 rescued by the addition of cysteine, methionine, or sodium sulfate. These findings strongly
643 implicate that *de novo* biosynthesis of sulfur-containing amino acids is a critical
644 downstream effector of glycolytic activity in promoting pseudohyphal differentiation under
645 nitrogen limitation. To directly assess the role of sulfur metabolism in fungal
646 morphogenesis, we generated and characterized knockout strains for key genes involved
647 in the sulfur assimilation pathway (*met32*, *met3*, *met16*, *met5*, *met10*, *met17*, *met2*,
648 and *met13*). The deletion of each of these genes resulted in substantial defects in
649 pseudohyphal differentiation under nitrogen-limiting conditions, directly implicating the
650 role of sulfur metabolism in regulating fungal morphogenesis. Remarkably, our sulfur add-
651 back experiments demonstrated that the ability of cysteine, methionine, or sodium sulfate
652 to rescue the morphogenetic defects exhibited by the aforesaid knockout strains was
653 dependent on the specific gene deleted and its position in the sulfur assimilation pathway,
654 aligning with the known biochemical functions of these enzymes [65], further solidifying
655 the direct involvement of sulfur metabolism in this morphogenetic switching process. How
656 active sulfur metabolism contributes towards fungal morphogenesis is not yet understood
657 but given its critical requirement during this phenomenon, it would be an important
658 question to explore and will further our overall understanding of this important biological
659 phenomenon.
660
661 It is interesting to note that the expression of Met4p, the principal transcriptional regulator
662 of the *de novo* biosynthesis of sulfur-containing amino acids in *S. cerevisiae* along with
663 Met32p one of its cognate DNA-binding cofactors [66], are significantly downregulated
664 when glycolysis is perturbed. Given the obligate requirement of Met4p interaction with
665 DNA-binding proteins such as Met28p, Met32p, or Met31p, to elicit transcriptional
666 activation of the genes involved in the *de novo* biosynthesis of sulfur-containing amino
667 acids [67], the observed downregulation in both Met4p and Met32p levels likely
668 compromises the overall biosynthesis of sulfur-containing amino acids. This concurrent
669 downregulation could explain the attenuated expression of downstream genes involved in
670 the synthesis of methionine and cysteine. This suggests a novel regulatory mechanism
671 wherein the expression of Met4p/Met32p is coupled to glycolytic activity, under nitrogen-
672 limiting conditions. Given that sulfur metabolism is coupled to glycolysis in *C. albicans* as
673 well and contributes towards fungal morphogenesis, it is likely that this conserved
674 regulatory axis might be critical for fungal morphogenesis in a broad range of fungal

675 species. We will be exploring the possible mechanisms underlying this novel regulatory
676 mechanism, in our laboratory.
677
678 Intriguingly, our work extended these findings to the pathogenic fungus *C. albicans*,
679 revealing a conserved role for glycolysis-mediated sulfur metabolism in hyphal
680 differentiation, a key virulence attribute in this species [49–51]. We demonstrated
681 that glucose is critical for hyphal differentiation in *C. albicans* under nitrogen-limiting
682 conditions, with non-fermentable carbon sources like ethanol and glycerol failing to induce
683 this morphological switch. Similar to our observations in *S. cerevisiae*,
684 *C. albicans* exhibited glycolysis-dependent hyphal formation under nitrogen limitation,
685 which was inhibited by 2DG. Consistent with our findings in *S. cerevisiae*, RT-qPCR
686 analysis revealed a significant downregulation of genes involved in *de novo* biosynthesis
687 of sulfur-containing amino acids (*met32*, *met3, met14*, *met16, met5*
688 (*ecm17*), *met10*, *met17* (*met15*), and *cys3*) upon 2DG treatment in *C. albicans*.
689 Importantly, exogenous addition of cysteine and methionine rescued the hyphal
690 differentiation defects caused by 2DG in *C. albicans*, suggesting a conserved link between
691 glycolysis and sulfur metabolism in regulating morphogenesis. Furthermore, a
692 *C. albicans* strain lacking *pfk1,* displayed attenuated hyphal differentiation, which was
693 rescued by cysteine supplementation, mirroring our observations in *S. cerevisiae*. These
694 results clearly demonstrate that *de novo* biosynthesis of sulfur-containing amino acids is
695 a critical downstream effector of glycolytic activity in promoting hyphal differentiation
696 under nitrogen-limiting conditions, in *C. albicans* as well. Given that central carbon
697 metabolic pathways like glycolysis and sulfur assimilation pathway are broadly conserved
698 metabolic processes across a plethora of fungal species, it is possible that this novel
699 regulatory axis might play a crucial role in modulating fungal morphogenesis in multiple
700 fungal species and further studies are warranted to explore this. Finally, given the
701 established link between hyphal differentiation and *C. albicans* virulence, we explored the
702 impact of glycolytic perturbation on the pathogenicity of this fungus. The *ΔΔpfk1* strain
703 displayed significantly reduced survival within *murine* macrophages and attenuated
704 virulence in a *murine* model of systemic infection, as evidenced by increased host survival,
705 lower kidney fungal burden, and reduced tissue colonization. These findings underscore
706 the critical role of glycolysis, and by extension, the glycolysis-dependent sulfur
707 metabolism, in the virulence of *C. albicans*.
708
709 In conclusion, our study unveils a conserved metabolic network that orchestrates fungal
710 morphogenesis in response to nutrient availability. We demonstrate that active glycolysis,
711 fueled by fermentable carbon sources, plays a crucial role in regulating the *de novo*
712 biosynthesis of sulfur-containing amino acids, which in turn are essential for the
713 morphological transitions in both *S. cerevisiae* and *C. albicans* (Fig 7). The attenuation
714 of *C. albicans* virulence upon disruption of this pathway highlights the potential of
715 targeting specific fungal metabolic networks as a novel antifungal strategy. Future
716 research in our laboratory will focus on elucidating the precise molecular mechanisms by
717 which glycolytic intermediates or downstream signals regulate the expression of sulfur
718 metabolism pathway and how sulfur-containing amino acids contribute to the cellular
719 processes underlying fungal morphogenesis.

720

721

722

723 # Materials and Methods

724

725 **Yeast Strains:**

726 The prototrophic diploid strains, ∑1278b or CEN.PK were used in all the experiments
727 involving *S. cerevisiae*. The prototrophic diploid strain, SC5314 was exclusively used in all
728 the experiments involving *C. albicans*. The yeast strains used in this study are listed in S1
729 Table.

730 **Generation of *S. cerevisiae* Gene Knockout and Epitope-tagged Strains:**

731 A standard PCR-based technique was used to amplify resistance cassettes (G418, HygB,
732 or NAT) with flanking sequences in order to carry out gene deletions. The target gene was
733 then replaced by homologous recombination using the lithium acetate-based
734 transformation [68]. Similarly, C-terminal epitope-tagged yeast strains were generated
735 using a PCR-based technique. This involved amplifying resistance cassettes, flanked by
736 sequences homologous to the C-terminal region of the target gene, along with the desired
737 epitope tags. The targeted gene was then tagged at its C-terminus through homologous
738 recombination, using the lithium acetate-based transformation method. Primers used for
739 these experiments are listed in S2 Table.

740 **Generation of *C. albicans* Gene Knockout Strains:**

741 The *C. albicans* strains used in this study are listed in S1 Table. The previously established
742 SAT1-flipper method was used with some modifications, for the deletion of the desired
743 genes [48]. To generate the *pfk1* deletion (*ΔΔpfk1*) strain, a DNA fragment carrying the
744 flanking regions of *pfk1* (100 bps homology) and the *SAT1*-flipper cassette was
745 transformed into *C. albicans* wild-type SC5314, using electroporation. Transformants were
746 selected based on their nourseothricin resistance. PCR confirmation was used to validate
747 the transformants. The *SAT1*-flipper cassette was then excised from the *pfk1* locus by
748 growing the cells in YPM medium (10g/l yeast extract, 20g/l peptone, and 2% (w/v)
749 maltose) to induce expression of the *MAL2* promoter-regulated recombinase. To knock out
750 the second allele of *pfk1*, the heterozygous *pfk1* deletion mutants (*Δpfk1/PFK1)* were used
751 for the transformation wherein the DNA fragment carrying the flanking regions of *pfk1*
752 (100 bps homology) and the *SAT1*-flipper cassette was transformed into *C. albicans*
753 *Δpfk1/PFK1* SC5314. Transformants were selected based on their nourseothricin
754 resistance. PCR confirmation was used to validate the transformants. Primers used to
755 generate or confirm the deletion strains are listed in S2 Table.

756 **Media and Growth Conditions:**

757 YPD broth containing 10g/l yeast extract, 20g/l peptone and 2% (w/v) glucose was used
758 for the overnight growth of the cultures. Nitrogen-limiting medium containing 1.7g/l yeast
759 nitrogen base without amino acids or ammonium sulfate, 2% (w/v) glucose (SLAD) or
760 various different fermentable or non-fermentable carbon sources, 50μM ammonium
761 sulfate and 2% (w/v) agar which was extensively washed, to remove excess nitrogen [15]
762 was used for all experiments involving pseudohyphal or hyphal differentiation. Overnight
763 cultures of various strains were grown in YPD broth and incubated at 30 °C with continuous
764 shaking at 200 rotations per minute (RPM). Reagents and tools used in this study are
765 mentioned in S3 Table.

766 **Pseudohyphal Differentiation Assay:**

767 To induce pseudohyphal differentiation in *S. cerevisiae,* overnight cultures of various
768 strains (listed in S1 Table) were spotted on nitrogen-limiting medium (SLA) containing 2%
769 glucose (SLAD). To examine the effect of various fermentable and non-fermentable carbon
770 sources on pseudohyphal differentiation, *S. cerevisiae* wild-type ∑1278b was spotted on
771 SLA (1.7g/l yeast nitrogen base without amino acids or ammonium sulfate, 2% (w/v)
772 washed agar and 50μM ammonium sulfate) containing either 2% (w/v) concentration of
773 glucose, sucrose, maltose, trehalose, fructose, mannose, galactose, ethanol, glycerol or
774 1% (w/v) concentration of acetate or 1mM DL-glyceraldehyde. In order to check the effect
775 of glycolysis inhibitors, 2-Deoxy-D-Glucose (2DG) and sodium citrate (NaCi), on
776 pseudohyphal differentiation, wild-type was spotted on SLAD containing sub-inhibitory
777 concentrations of 2DG or NaCi. Plates were incubated for 10 days at 30 °C. After 10 days,
778 imaging was done using Olympus MVX10 stereo microscope. Cells from colonies were
779 isolated and single cells were imaged using Zeiss Apotome microscope and the percentage
780 of pseudohyphal cells was calculated using ImageJ. Cells with a length/width ratio of 2 or
781 more were considered as pseudohyphal cells as described previously [22]. Statistical
782 analysis was done using unpaired t-test. Error bars represent SEM. All the experiments
783 were replicated minimally thrice with technical replicates.

784 **Hyphal Differentiation Assay:**

785 To induce hyphal differentiation in *C. albicans,* overnight cultures of each strain (listed in
786 S1 Table) were spotted on nitrogen-limiting medium (SLAD). To examine the effect of
787 various carbon sources on hyphal differentiation, *C. albicans* wild-type SC5314 was
788 spotted on SLA medium (1.7g/l yeast nitrogen base without amino acids or ammonium
789 sulfate, 2% (w/v) agar and 50μM ammonium sulfate) containing 2% (w/v) concentration
790 of each carbon source (glucose, ethanol and glycerol). To check the effect of glycolysis
791 inhibitor, 2-Deoxy-D-Glucose (2DG) on hyphal differentiation, wild-type was spotted on
792 SLAD containing sub-inhibitory concentration of 2DG. All the plates were incubated for 7
793 days at 37 °C. After 7 days, cells from colonies were isolated and single cells were imaged
794 using Zeiss Apotome microscope and percentage of hyphal cells was calculated using
795 ImageJ. Cells with a length/width ratio of 4.5 or more were considered as hyphal cells as
796 described previously [44]. Statistical analysis was done using unpaired t-test. Error bars
797 represent SEM. All the experiments were replicated minimally thrice with technical
798 replicates.

799 **Spot Dilution Assays:**

800 A spot dilution assay was performed to investigate the effect of the gene deletions or the
801 effect of the glycolysis inhibitors (2DG or NaCi) on the overall growth of specific strains.
802 Respected strains were grown in YPD liquid medium at 30 °C with shaking at 200 rpm,
803 overnight. To monitor the growth of wild-type strains (∑1278b or CEN.PK) on SLAD,
804 SLAD+2DG and SLAD+NaCi, serial dilutions (U-Undiluted, 10^{-1}-1:10 dilution, 10^{-2}-1:100
805 dilution, 10^{-3}-1:1000 dilution, 10^{-4}-1:10000 dilution) were prepared and spotted on SLAD,
806 SLAD+2DG and SLAD+NaCi. To monitor the growth of deletion strains (listed in S1 Table)
807 on SLAD, serial dilutions (U-Undiluted, 10^{-1}-1:10 dilution, 10^{-2}-1:100 dilution, 10^{-3}-1:1000
808 dilution, 10^{-4}-1:10000 dilution) were prepared for each strain along with wild-type strains
809 and spotted on SLAD. The plates were incubated at 30 °C for 48 hours before imaging. All
810 the experiments were replicated minimally thrice.

811 **Sulfur Add-back Assays:**

812 In order to perform sulfur add-back assays, overnight cultures of various strains of
813 *S. cerevisiae* or *C. albicans* (listed in S1 Table) were spotted on SLAD or SLAD containing
814 sub-inhibitory concentration of 2DG, in the presence and absence of sulfur-containing
815 compounds including cysteine, methionine or sodium sulfate. Plates were incubated for 10
816 days at 30 °C to induce pseudohyphal differentiation in *S. cerevisiae*. After 10 days,
817 imaging was done using Olympus MVX10 stereo microscope. Cells from colonies were
818 isolated and single cells were imaged using Zeiss Apotome microscope and percentage of
819 pseudohyphal cells were calculated using ImageJ. For hyphal differentiation assays in
820 *C. albicans*, plates were incubated for 7 days at 37 °C. After 7 days, cells from colonies
821 were isolated and single cells were imaged using Zeiss Apotome microscope and
822 percentage of hyphal cells were calculated using ImageJ. Statistical analysis was done
823 using unpaired t-test. Error bars represent SEM. All the experiments were replicated
824 minimally thrice with technical replicates.

825 **RNA-Sequencing:**

826 **Sample Collection.** Overnight culture of *S. cereviae* wild-type ∑1278b was spotted on
827 nitrogen-limiting media containing 2% (w/v) glucose (SLAD) with and without sub-
828 inhibitory concentration of 2-Deoxy-D-Glucose (2DG). The plates were incubated at 30 °C
829 and colonies were isolated on day 5 (D-5) and day 10 (D-10).

830 **RNA-Extraction.** Total RNA from the sample was extracted using the protocol mentioned
831 in the Ribopure RNA purification kit (yeast) (cat. #AM1926). Following a DNAse treatment
832 to eliminate any genomic DNA from the sample, the extracted RNA was submitted to the
833 CCMB next-generation sequencing facility for RNA-Seqencing. The NovaSeq 6000
834 equipment was used to sequence transcriptomes.

835 **RNA-Sequencing Analysis.** Raw sequencing reads were obtained in FASTQ format. The
836 reference genome and annotation files for the *S. cerevisiae* strain ∑1278b were
837 downloaded from the Saccharomyces Genome Database (SGD). Quality assessment of the
838 raw reads was performed using FastQC (version 0.12.1). Adapter sequences were trimmed
839 using Cutadapt (version 4.6). The reference genome was indexed with Hisat2 (version
840 2.2.1), and Samtools (version 1.20) was used to filter out multi-mapped reads and convert
841 SAM files to BAM format. Read counting for uniquely mapped reads was done with
842 FeatureCounts, using gene annotation data from the reference *S. cerevisiae* ∑1278b
843 genome. Normalization and differential gene expression analysis were performed using
844 R (version 4.3.2). Genes with a $\log_2$ fold change of ≥1 were considered to be upregulated,
845 indicating at least a doubling in expression under the given condition, while those with a
846 $\log_2$ fold change of ≤ -1 were considered to be downregulated.

847 **Protein Isolation:**

848 For Western blotting experiments, in order to isolate proteins from liquid cultures,
849 overnight yeast cultures were back-diluted in 10 ml of liquid SLAD in the presence and
850 absence of 2-Deoxy-D-Glucose (2DG). The yeast cells were grown till an OD_{600} of ~1 and
851 cells were harvested by centrifugation at 3000 rpm for 10 minutes at room temperature
852 (RT). To isolate proteins from colonies, overnight cultures of pertinent strains were spotted
853 on SLAD with and without sub-inhibitory concentration of 2-Deoxy-D-Glucose (2DG) and
854 colonies were isolated and resuspended in 1ml of 1X PBS (Phosphate Buffered Saline) after
855 5 days (D-5). Cells were harvested by centrifugation at 14000 rpm for 10 minutes at room
856 temperature. Pelleted cells (from liquid cultures and colonies) were resuspended in 300µl
857 of ice cold 10% (w/v) TCA solution and disrupted using bead-beating by addition of 150µl

858 of glass beads at 4°C. Supernatant was transferred to another tube. Next, proteins were
859 pelleted by centrifugation at 14,000 rpm for 10 minutes at 4°C and supernatant was
860 discarded. Each pellet was resuspended in 400µl of SDS/glycerol buffer (7.3% (w/v) SDS,
861 29% (v/v) glycerol and 83.3mM tris-base) and boiled at 95°C for 10 minutes with
862 occasional vortexing followed by centrifugation at 14,000 rpm for 10 minutes at room
863 temperature. Supernatant was transferred to a fresh tube and used for protein estimation
864 using BCA protein estimation kit (cat. #23227). Finally, all samples were diluted in SDS-
865 PAGE loading buffer (100mM Tris-Cl, 4% (w/v) SDS, 0.02% (w/v) bromophenol blue, 20%
866 (w/v), glycerol and 7.5% (v/v) β-mercaptoethanol) and heated for 5 minutes at 90°C.

867 **Immunodetection:**

868 Protein samples were separated using SDS-PAGE on polyacrylamide gels and transferred
869 to PVDF membranes with a Mini Trans-Blot Cell module (Bio-Rad). The membranes were
870 blocked for 1 hour at room temperature with 5% (w/v) non-fat dry milk in 1X TBST buffer
871 (20 mM Tris-Base, pH 7.6, 150 mM NaCl, 0.1% (v/v) Tween-20) with gentle orbital
872 shaking. After blocking, the membranes were incubated overnight at 4°C with primary
873 antibodies (1:2000 dilution) in 1X TBST buffer containing 5% (w/v) non-fat dry milk.
874 Following this, the membranes were washed three times for 10 minutes in 1X TBST and
875 then incubated for 1 hour at room temperature with HRP-conjugated secondary antibodies
876 (1:4000 dilution) in 1X TBST with 5% (w/v) non-fat dry milk. After three additional washes
877 in 1X TBST, chemiluminescent substrate was added and bands were detected using the
878 SuperSignal West chemiluminescent substrate (cat. #34579, cat. #34094) and visualized
879 using the Bio-Rad ChemiDoc™MP imaging system.

880 **Antibodies:**

881 HA-Tag (C29F4) Rabbit mAb (cat. #3724), β-actin (8H10D10) Mouse mAb (cat. #3700),
882 Goat anti-Rabbit IgG-HRP conjugate (cat. #7074) and Horse anti-Mouse IgG-HRP
883 conjugate (cat. #7076) were purchased from Cell Signaling Technology. Pgk1 Mouse mAb
884 (cat. #sc-130335) was purchased from Santa Cruz Biotechnology.

885 **Densitometric Analysis:**

886 Raw images of western blots were analysed using ImageJ to normalize target protein
887 expression with the expression of housekeeping proteins including PGK1 and β-actin in
888 order to make densitometric graphs. Statistical analysis was done using unpaired t-test,
889 with error bars representing SEM. All the experiments were replicated minimally thrice.

890 **Quantitative Real Time Polymerase Chain Reaction (RT-qPCR) Assay:**

891 Overnight cultures of *C. albicans* wild-type SC5314 was spotted on SLAD with and without
892 sub-inhibitory concentration of 2-Deoxy-D-Glucose (2DG) and plates were incubated at
893 37 °C for 4 days. After 4 days, colonies were isolated and total RNA was extracted using
894 the protocol mentioned in the Ribopure RNA purification kit, yeast (cat. #AM1926). cDNA
895 synthesis was carried out using PrimeScript cDNA synthesis kit (cat. #6110A). Primers
896 used for RT-qPCR were designed using PrimeQuest tool of Integrated DNA Technologies
897 (IDT). RT-qPCR was performed using iTaq Universal SYBR green mastermix (cat.
898 #1725121). Actin was used as housekeeping gene for normalization. The results were
899 analysed using the $2^{-\Delta\Delta CT}$ method [69] and statistical analysis was done using unpaired t-
900 test, with error bars representing SEM. All the experiments were replicated minimally
901 thrice with technical replicates. Primers used in the RT-qPCR experiments are mentioned
902 in S2 Table.

903 ***Ex vivo* Microbial Survival Assay:**

904 *Ex vivo* microbial survival assay in macrophages was conducted as described in previous
905 studies with some modifications [70,71]. *RAW 264.7* macrophages (1×10^6 cells) were
906 cultured in six-well plates with DMEM supplemented with 10% FBS. After 16 hours of
907 incubation, the cells were treated with *C. albicans* wild-type SC5314 or *ΔΔpfk1* at a
908 multiplicity of infection (MOI) of 10, for 1 hour in antibiotic-free DMEM containing 10%
909 FBS. The media was then removed, and the cells were washed six times with 1X PBS to
910 eliminate any free, non-phagocytosed fungal cells. Next, the cells were lysed with 350 µl
911 of lysis buffer containing 0.025% SDS in 1X PBS. The lysate volume was adjusted to 1 ml
912 with 1X PBS, and a 100 µl undiluted aliquot was plated on YPD agar plate. Serial dilutions
913 of the lysate were also plated on YPD agar plates. These plates were incubated overnight
914 at 37 °C. The following day, colony-forming units (CFUs) were counted and plotted. The
915 percentage of survival was calculated as the number of CFUs in the presence of
916 macrophages divided by the number of CFUs in the absence of macrophages. Statistical
917 analysis was done using unpaired t-test, with error bars representing SEM. All the
918 experiments were replicated minimally thrice.

919 ***In vivo Murine* Model of Systemic Candidiasis**

920 *In vivo* infection experiments were performed as previously described [72]. Briefly,
921 *C. albicans* wild-type SC5314 and *ΔΔpfk1* were grown overnight in YPD medium at 30 °C.
922 The overnight cultures were back-diluted in 10 ml of YPD liquid medium and allowed to
923 grow till and OD of ~0.6, then washed and resuspended at concentration of 1×10^7 CFU/ml
924 in 1X PBS. C57BL/6 wild-type mice, aged 6 to 8 weeks, were injected intravenously *via*
925 lateral tail vein with *C. albicans* wild-type SC5314 or *ΔΔpfk1* at a concentration of 1×10^7
926 CFU/ml. After infection, mice were monitored for survival and daily for signs of morbidity
927 and mortality were recorded over a period of 21 days. Survival data were analysed using
928 the Log-rank Mantel-Cox test with GraphPad Prism.

929 **Determination of Fungal Burden:**

930 To assess fungal burden, mice injected with *C. albicans* wild-type SC5314 or *ΔΔpfk1* were
931 sacrificed at ~2 days and kidneys were harvested from infected mice. Kidneys were
932 weighed and then homogenized using a sterilized and PBS-washed Dounce homogenizer
933 (cat. #D8938). Kidney suspensions were then diluted in 1 ml of 1X PBS and serially diluted.
934 Then 100µl of dilutions was plated on YPD agar plates and allowed to grow at 37 °C. Colony
935 forming units were calculated by the following formula: (number of colonies × dilution
936 factor × 10)/organ weight in grams (g). Statistical analysis was done using unpaired
937 t-test. Error bars represent SEM. All the experiments were replicated minimally thrice.

938 **Histopathology:**

939 For histopathological examination, kidneys were collected and fixed in 10% neutral
940 buffered formalin for about two weeks. After fixation, the kidneys were processed,
941 embedded in paraffin, and sectioned to 4 µm thickness. The tissue sections were then
942 stained using the GMS stain (Grocott Methenamine Silver stain) and the protocol
943 mentioned in the GMS staining kit manual (cat. #AB287884) was followed.

944 **Illustrations:**

945 Figure illustrations were created using Biorender (https://app.biorender.com).

946

Author Contributions

Dhrumi Shah: Conceptualization; Investigation; Formal analysis; Visualization; Writing-original draft. **Adishree M:** Investigation. **Nikita Rewatkar:** Investigation. **Siddhi Gupta:** Investigation. **Sudharsan Mathivathanan:** Investigation. **Sriram Varahan:** Conceptualization; Supervision; Funding acquisition; Investigation; Formal analysis; Visualization; Writing-original draft; Writing-review and editing.

Acknowledgements

We gratefully acknowledge the invaluable support and resources offered by CSIR-Centre for Cellular and Molecular Biology (CCMB) central facilities including Advanced Microscopy and Imaging facility (AMIF), Next Generation Sequencing (NGS) facility and Animal House facility. We acknowledge help from T. Avinash Raj (CSIR- CCMB) for preparation of samples for histological analysis. DS thanks University Grants Commission (UGC), India for their research fellowship. SV acknowledges funding from Indian Council of Medical Research (ICMR) (IIRPSG-2024-01-02717), India; Anusandhan National Research Foundation (ANRF) (SRG/2023/000470), India; Council of Scientific & Industrial Research (CSIR) (FTT070505), India; and DBT-Wellcome Trust India Alliance (IA/E/16/1/502996), India.

Conflict of Interest

The authors declare that they have no conflict of interests.

984 **References**

985 1. Lin X, Andrew Alspaugh J, Liu H, Harris S. Fungal morphogenesis. Cold Spring Harb Perspect
986 Med. 2015. doi:10.1101/cshperspect.a019679

987 2. Gow NAR, Brown AJP, Odds FC. Fungal morphogenesis and host invasion. Current Opinion in
988 Microbiology. 2002. doi:10.1016/S1369-5274(02)00338-7

989 3. Naranjo-Ortiz MA, Gabaldón T. Fungal evolution: major ecological adaptations and
990 evolutionary transitions. Biol Rev. 2019. doi:10.1111/brv.12510

991 4. Wang L, Lin X. Morphogenesis in Fungal Pathogenicity: Shape, Size, and Surface. PLoS
992 Pathog. 2012. doi:10.1371/journal.ppat.1003027

993 5. Min K, Neiman AM, Konopka JB. Fungal Pathogens: Shape-Shifting Invaders. Trends in
994 Microbiology. 2020. doi:10.1016/j.tim.2020.05.001

995 6. Puumala E, Fallah S, Robbins N, Cowen LE. Advancements and challenges in antifungal
996 therapeutic development. Clinical Microbiology Reviews. 2024. doi:10.1128/cmr.00142-23

997 7. Sexton AC, Howlett BJ. Parallels in fungal pathogenesis on plant and animal hosts. Eukaryotic
998 Cell. 2006. doi:10.1128/EC.00277-06

999 8. Christensen M. A View of Fungal Ecology. Mycologia. 1989.
1000 doi:10.1080/00275514.1989.12025620

1001 9. Riquelme M, Aguirre J, Bartnicki-García S, Braus GH, Feldbrügge M, Fleig U, et al. Fungal
1002 Morphogenesis, from the Polarized Growth of Hyphae to Complex Reproduction and Infection
1003 Structures. Microbiol Mol Biol Rev. 2018. doi:10.1128/mmbr.00068-17

1004 10. Nantel A, Dignard D, Bachewich C, Harcus D, Marcil A, Bouin AP, et al. Transcription profiling
1005 of *Candida albicans* cells undergoing the yeast-to-hyphal transition. Mol Biol Cell. 2002.
1006 doi:10.1091/mbc.E02-05-0272

1007 11. Ryan O, Shapiro RS, Kurat CF, Mayhew D, Baryshnikova A, Chin B, et al. Global gene deletion
1008 analysis exploring yeast filamentous growth. Science (80-). 2012.
1009 doi:10.1126/science.1224339

1010 12. Fleck CB, Schöbel F, Brock M. Nutrient acquisition by pathogenic fungi: Nutrient availability,
1011 pathway regulation, and differences in substrate utilization. International Journal of Medical
1012 Microbiology. 2011. doi:10.1016/j.ijmm.2011.04.007

1013 13. Kumar A. The Complex Genetic Basis and Multilayered Regulatory Control of Yeast
1014 Pseudohyphal Growth. Annual Review of Genetics. 2021. doi:10.1146/annurev-genet-
1015 071719-020249

1016 14. Broach JR. Nutritional control of growth and development in yeast. Genetics. 2012.
1017 doi:10.1534/genetics.111.135731

1018 15. Gimeno CJ, Ljungdahl PO, Styles CA, Fink GR. Unipolar cell divisions in the yeast *S. cerevisiae*
1019 lead to filamentous growth: Regulation by starvation and RAS. Cell. 1992. doi:10.1016/0092-
1020 8674(92)90079-R

1021 16. Csank C, Schröppel K, Leberer E, Harcus D, Mohamed O, Meloche S, et al. Roles of the
1022 *Candida aibicans* mitogen-activated protein kinase homolog, Cek1p, in hyphal development
1023 and systemic candidiasis. Infect Immun. 1998. doi:10.1128/iai.66.6.2713-2721.1998

1024 17. Thompson DS, Carlisle PL, Kadosh D. Coevolution of morphology and virulence in *Candida*
1025 species. Eukaryotic Cell. 2011. doi:10.1128/EC.05085-11

1026 18. Palková Z, Váchová L. Life within a community: Benefit to yeast long-term survival. FEMS
1027 Microbiology Reviews. 2006. doi:10.1111/j.1574-6976.2006.00034.x

1028 19. Pan X, Harashima T, Heitman J. Signal transduction cascades regulating pseudohyphal
1029 differentiation of *Saccharomyces cerevisiae*. Current Opinion in Microbiology. 2000.
1030 doi:10.1016/S1369-5274(00)00142-9

1031 20. Gancedo JM. Yeast Carbon Catabolite Repression. Microbiol Mol Biol Rev. 1998.
1032 doi:10.1128/mmbr.62.2.334-361.1998

1033 21. Lorenz MC. Yeast pseudohyphal growth is regulated by GPA2, a G protein alpha homolog.
1034 EMBO J. 1997. doi:10.1093/emboj/16.23.7008

1035 22. Schröder M, Chang JS, Kaufman RJ. The unfolded protein response represses nitrogen-
1036 starvation induced developmental differentiation in yeast. Genes Dev. 2000.
1037 doi:10.1101/gad.852300

1038 23. De Deken RH. The Crabtree effect: a regulatory system in yeast. J Gen Microbiol. 1966.
1039 doi:10.1099/00221287-44-2-149

1040 24. Barford JP, Hall RJ. An examination of the crabtree effect in *Saccharomyces cerevisiae*: The
1041 role of respiratory adaptation. J Gen Microbiol. 1979. doi:10.1099/00221287-114-2-267

1042 25. Cramer FB, Woodward GE. 2-Desoxy-D-glucose as an antagonist of glucose in yeast
1043 fermentation. J Franklin Inst. 1952. doi:10.1016/0016-0032(52)90852-1

1044 26. Yoshino M, Murakami K. AMP deaminase as a control system of glycolysis in yeast. Mechanism
1045 of the inhibition of glycolysis by fatty acid and citrate. J Biol Chem. 1982. doi:10.1016/s0021-
1046 9258(18)33871-7

1047 27. Laxman S, Tu BP. Multiple TORC1-associated proteins regulate nitrogen starvation-dependent
1048 cellular differentiation in *Saccharomyces cerevisiae*. PLoS One. 2011.
1049 doi:10.1371/journal.pone.0026081

1050 28. Heinisch J. Construction and physiological characterization of mutants disrupted in the
1051 phosphofructokinase genes of *Saccharomyces cerevisiae*. Curr Genet. 1986.
1052 doi:10.1007/BF00420611

1053 29. Smith MG, Des Etages SG, Snyder M. Microbial Synergy via an Ethanol-Triggered Pathway.
1054 Mol Cell Biol. 2004. doi:10.1128/mcb.24.9.3874-3884.2004

1055 30. Foy JJ, Bhattacharjee JK. Biosynthesis and regulation of fructose-1,6-bisphosphatase and
1056 phosphofructokinase in *Saccharomyces cerevisiae* grown in the presence of glucose and
1057 gluconeogenic carbon sources. J Bacteriol. 1978. doi:10.1128/jb.136.2.647-656.1978

1058 31. Bennetzen JL, Hall BD. The primary structure of the *Saccharomyces cerevisiae* gene for
1059 alcohol dehydrogenase. J Biol Chem. 1982. doi:10.1016/s0021-9258(19)81067-0

1060 32. Wu Y, Zhang S, Gong X, Yu Q, Zhang Y, Luo M, et al. Glycolysis regulates gene expression
1061 by promoting the crosstalk between H3K4 trimethylation and H3K14 acetylation in
1062 *Saccharomyces cerevisiae*. J Genet Genomics. 2019. doi:10.1016/j.jgg.2019.11.007

1063 33. Newcomb LL, Diderich JA, Slattery MG, Heideman W. Glucose regulation of *Saccharomyces*
1064 *cerevisiae* cell cycle genes. Eukaryot Cell. 2003. doi:10.1128/EC.2.1.143-149.2003

1065 34. Martíez-force E, Benítez T. Changes in yeast amino acid pool with respiratory versus
1066 fermentative metabolism. Biotechnol Bioeng. 1992. doi:10.1002/bit.260400602

1067 35. Dikicioglu D, Karabekmez E, Rash B, Pir P, Kirdar B, Oliver SG. How yeast re-programmes its
1068 transcriptional profile in response to different nutrient impulses. BMC Syst Biol. 2011.
1069 doi:10.1186/1752-0509-5-148

1070 36. Wu J, Zhang N, Hayes A, Panoutsopoulo K, Oliver SG. Global analysis of nutrient control of
1071 gene expression in *Saccharomyces cerevisiae* during growth and starvation. Proc Natl Acad
1072 Sci U S A. 2004. doi:10.1073/pnas.0308321100

1073 37. Masselot M, Surdin-Kerjan Y. Methionine biosynthesis in *Saccharomyces cerevisiae*. Mol Gen
1074 Genet MGG. 1977. doi:10.1007/bf00265572

1075 38. Masselot M, de Robichon-Szulmajster H. Methionine biosynthesis in *Saccharomyces*
1076 *cerevisiae* - I. Genetical analysis of auxotrophic mutants. MGG Mol Gen Genet. 1975.
1077 doi:10.1007/BF00264692

1078 39. Kinzurik MI, Ly K, David KM, Gardner RC, Fedrizzi B. The GLO1 Gene Is Required for Full
1079 Activity of O-Acetyl Homoserine Sulfhydrylase Encoded by MET17. ACS Chem Biol. 2017.
1080 doi:10.1021/acschembio.6b00815

1081 40. Yamagata S. Partial purification and some properties of homoserine O-acetyltransferase of a

1082 methionine auxotroph of *Saccharomyces cerevisiae*. J Bacteriol. 1987.
1083 doi:10.1128/jb.169.8.3458-3463.1987

1084 41. Raymond RK, Kastanos EK, Appling DR. *Saccharomyces cerevisiae* expresses two genes
1085 encoding isozymes of methylenetetrahydrofolate reductase. Arch Biochem Biophys. 1999.
1086 doi:10.1006/abbi.1999.1498

1087 42. Huang G. Regulation of phenotypic transitions in the fungal pathogen *Candida albicans*.
1088 Virulence. 2012. doi:10.4161/viru.20010

1089 43. Askew C, Sellam A, Epp E, Hogues H, Mullick A, Nantel A, et al. Transcriptional regulation of
1090 carbohydrate metabolism in the human pathogen *Candida albicans*. PLoS Pathog. 2009.
1091 doi:10.1371/journal.ppat.1000612

1092 44. Su C, Yu J, Sun Q, Liu Q, Lu Y. Hyphal induction under the condition without inoculation in
1093 *Candida albicans* is triggered by Brg1-mediated removal of NRG1 inhibition. Mol Microbiol.
1094 2018. doi:10.1111/mmi.13944

1095 45. Chebaro Y, Lorenz M, Fa A, Zheng R, Gustin M. Adaptation of *Candida albicans* to reactive
1096 sulfur species. Genetics. 2017. doi:10.1534/genetics.116.199679

1097 46. Shrivastava M, Feng J, Coles M, Clark B, Islam A, Dumeaux V, et al. Modulation of the complex
1098 regulatory network for methionine biosynthesis in fungi. Genetics. 2021.
1099 doi:10.1093/GENETICS/IYAA049

1100 47. Li DD, Wang Y, Dai B Di, Li XX, Zhao LX, Cao YB, et al. ECM17-dependent methionine/cysteine
1101 biosynthesis contributes to biofilm formation in *Candida albicans*. Fungal Genet Biol. 2013.
1102 doi:10.1016/j.fgb.2012.11.010

1103 48. Reuß O, Vik Å, Kolter R, Morschhäuser J. The SAT1 flipper, an optimized tool for gene
1104 disruption in *Candida albicans*. Gene. 2004. doi:10.1016/j.gene.2004.06.021

1105 49. Gow NAR, Van De Veerdonk FL, Brown AJP, Netea MG. *Candida albicans* morphogenesis and
1106 host defence: Discriminating invasion from colonization. Nature Reviews Microbiology. 2012.
1107 doi:10.1038/nrmicro2711

1108 50. Moyes DL, Wilson D, Richardson JP, Mogavero S, Tang SX, Wernecke J, et al. Candidalysin is
1109 a fungal peptide toxin critical for mucosal infection. Nature. 2016. doi:10.1038/nature17625

1110 51. Wilson D, Naglik JR, Hube B. The Missing Link between *Candida albicans* Hyphal
1111 Morphogenesis and Host Cell Damage. PLoS Pathogens. 2016.
1112 doi:10.1371/journal.ppat.1005867

1113 52. Jiménez-López C, Lorenz MC. Fungal Immune Evasion in a Model Host-Pathogen Interaction:
1114 *Candida albicans* Versus Macrophages. PLoS Pathog. 2013.
1115 doi:10.1371/journal.ppat.1003741

1116 53. Uwamahoro N, Verma-Gaur J, Shen HH, Qu Y, Lewis R, Lu J, et al. The pathogen *Candida*
1117 *albicans* hijacks pyroptosis for escape from macrophages. MBio. 2014.
1118 doi:10.1128/mBio.00003-14

1119 54. May RC, Casadevall A. In fungal intracellular pathogenesis, form determines fate. MBio. 2018.
1120 doi:10.1128/mbio.02092-18

1121 55. Hirayama T, Miyazaki T, Ito Y, Wakayama M, Shibuya K, Yamashita K, et al. Virulence
1122 assessment of six major pathogenic *Candida* species in the mouse model of invasive
1123 candidiasis caused by fungal translocation. Sci Rep. 2020. doi:10.1038/s41598-020-60792-
1124 y

1125 56. Segal E, Frenkel M. Experimental in vivo models of Candidiasis. Journal of Fungi. 2018.
1126 doi:10.3390/jof4010021

1127 57. Lionakis MS, Lim JK, Lee CCR, Murphy PM. Organ-specific innate immune responses in a
1128 mouse model of invasive candidiasis. J Innate Immun. 2011. doi:10.1159/000321157

1129 58. Pappas PG, Lionakis MS, Arendrup MC, Ostrosky-Zeichner L, Kullberg BJ. Invasive
1130 candidiasis. Nat Rev Dis Prim. 2018. doi:10.1038/nrdp.2018.26

1131 59. Turcotte B, Liang XB, Robert F, Soontorngun N. Transcriptional regulation of nonfermentable
1132 carbon utilization in budding yeast. FEMS Yeast Research. 2010. doi:10.1111/j.1567-
1133 1364.2009.00555.x

1134 60. Kubota S, Takeo I, Kume K, Kanai M, Shitamukai A, Mizunuma M, et al. Effect of ethanol on
1135 cell growth of budding yeast: Genes that are important for cell growth in the presence of
1136 ethanol. Biosci Biotechnol Biochem. 2004. doi:10.1271/bbb.68.968

1137 61. Kraakman L, Lemaire K, Ma P, Teunlssen AWRH, Donaton MCV, Van Dijck P, et al. A
1138 *Saccharomyces cerevisiae* G-protein coupled receptor, Gpr1, is specifically required for
1139 glucose activation of the cAMP pathway during the transition to growth on glucose. Mol
1140 Microbiol. 1999. doi:10.1046/j.1365-2958.1999.01413.x

1141 62. Yun CW, Tamaki H, Nakayama R, Yamamoto K, Kumagai H. G-protein coupled receptor from
1142 yeast *Saccharomyces cerevisiae*. Biochem Biophys Res Commun. 1997.
1143 doi:10.1006/bbrc.1997.7649

1144 63. Lorenz MC, Pan X, Harashima T, Cardenas ME, Xue Y, Hirsch JP, et al. The G protein-coupled
1145 receptor Gpr1 is a nutrient sensor that regulates pseudohyphal differentiation in
1146 *Saccharomyces cerevisiae*. Genetics. 2000. doi:10.1093/genetics/154.2.609

1147 64. Gancedo JM. Control of pseudohyphae formation in *Saccharomyces cerevisiae* . FEMS
1148 Microbiol Rev. 2001. doi:10.1111/j.1574-6976.2001.tb00573.x

1149 65. Thomas D, Surdin-Kerjan Y. Metabolism of sulfur amino acids in *Saccharomyces cerevisiae*.
1150 Microbiol Mol Biol Rev. 1997. doi:10.1128/mmbr.61.4.503-532.1997

1151 66. Blaiseau P-L, Isnard A-D, Surdin-Kerjan Y, Thomas D. Met31p and Met32p, Two Related Zinc
1152 Finger Proteins, Are Involved in Transcriptional Regulation of Yeast Sulfur Amino Acid
1153 Metabolism. Mol Cell Biol. 1997. doi:10.1128/mcb.17.7.3640

1154 67. Blaiseau PL, Thomas D. Multiple transcriptional activation complexes tether the yeast
1155 activator Met4 to DNA. EMBO J. 1998. doi:10.1093/emboj/17.21.6327

1156 68. Schiestl RH, Gietz RD. High efficiency transformation of intact yeast cells using single
1157 stranded nucleic acids as a carrier. Curr Genet. 1989. doi:10.1007/BF00340712

1158 69. Winer J, Jung CKS, Shackel I, Williams PM. Development and validation of real-time
1159 quantitative reverse transcriptase-polymerase chain reaction for monitoring gene expression
1160 in cardiac myocytes in vitro. Anal Biochem. 1999. doi:10.1006/abio.1999.4085

1161 70. Netea MG, Van der Graaf CAA, Vonk AG, Verschueren I, Van der Meet JWM, Kullberg BJ. The
1162 role of toll-like receptor (TLR) 2 and TLR4 in the host defense against disseminated
1163 candidiasis. J Infect Dis. 2002. doi:10.1086/340511

1164 71. Pradhan B, Guha D, Ray P, Das D, Aich P. Comparative Analysis of the Effects of Two Probiotic
1165 Bacterial Strains on Metabolism and Innate Immunity in the RAW 264.7 *Murine* Macrophage
1166 Cell Line. Probiotics Antimicrob Proteins. 2016. doi:10.1007/s12602-016-9211-4

1167 72. Majer O, Bourgeois C, Zwolanek F, Lassnig C, Kerjaschki D, Mack M, et al. Type I interferons
1168 promote fatal immunopathology by regulating inflammatory monocytes and neutrophils
1169 during *Candida* infections. PLoS Pathog. 2012. doi:10.1371/journal.ppat.1002811

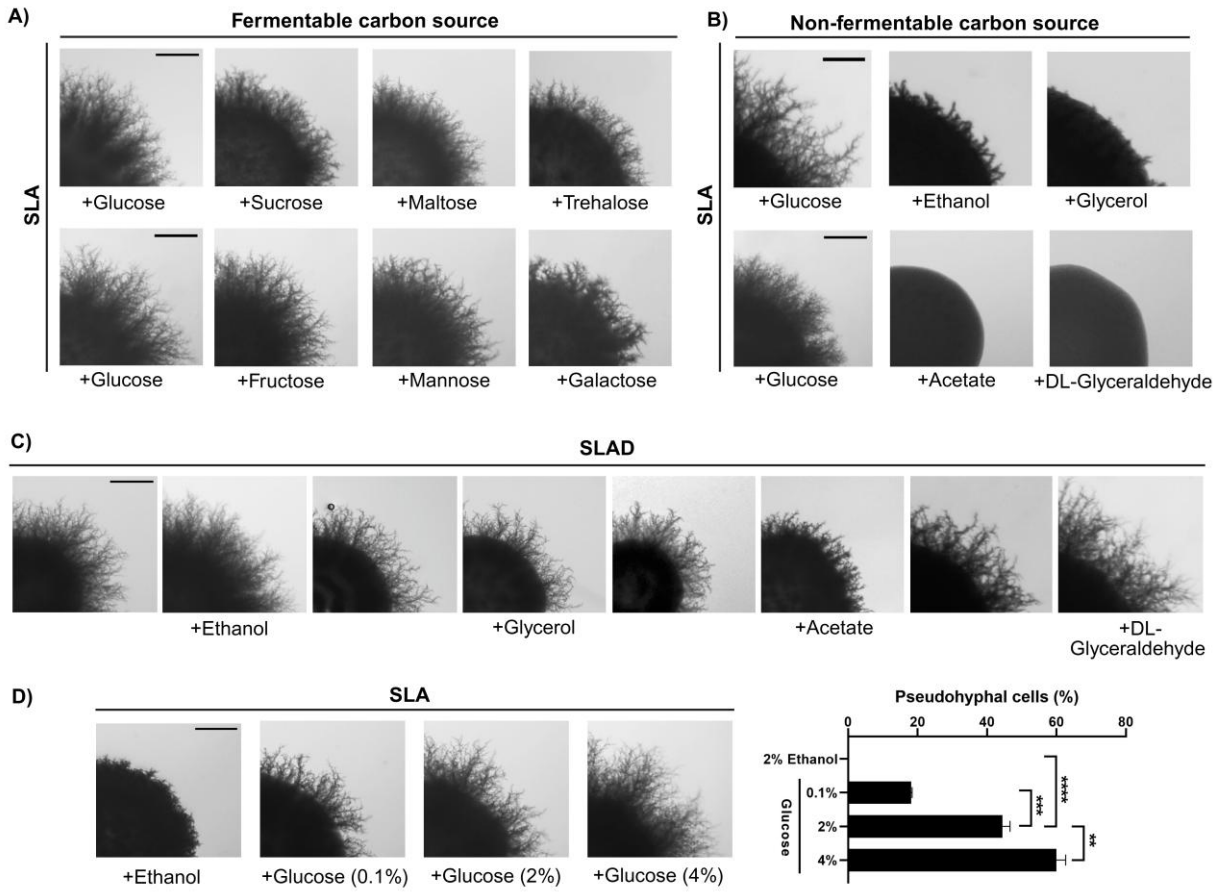

Fig 1. Quality and Quantity of Carbon Source Influences Fungal Morphogenesis

(A) Wild-type ∑1278b was spotted on nitrogen-limiting medium (SLA) containing fermentative carbon sources including glucose, sucrose, maltose, trehalose, fructose, mannose and galactose (each at 2% concentration) and imaged after 10 days of incubation at 30 °C, using Olympus MVX10 stereo microscope. Scale bar represents 1mm for whole colony images. **(B)** Wild-type ∑1278b was spotted on SLA containing non-fermentable carbon sources (ethanol (2%), glycerol (2%), acetate (1%) and DL-glyceraldehyde(1mM)) and imaged using Olympus MVX10 stereo microscope after 10 days of incubation at 30 °C. Scale bar represents 1mm for whole colony images. **(C)** Wild-type ∑1278b was spotted on SLA containing 2% glucose (SLAD), in the presence and absence of various non-fermentative carbon sources and imaged after 10 days of incubation at 30 °C, using Olympus MVX10 stereo microscope. Scale bar represents 1mm for whole colony images. **(D)** Wild-type ∑1278b was spotted on SLA with different concentrations of glucose ranging from 0.1% to 4% and SLA with ethanol (2%) was used as a negative control. After 10 days, imaging was done using Olympus MVX10 stereo microscope. Scale bar represents 1mm for whole colony images. Cells from colonies were isolated and single cells were imaged using Zeiss Apotome microscope and percentage of pseudohyphal cells were calculated using ImageJ. Statistical analysis was done using unpaired t-test, ****($P<0.0001$), ***($P<0.001$) and **($P<0.01$). Error bars represent SEM.

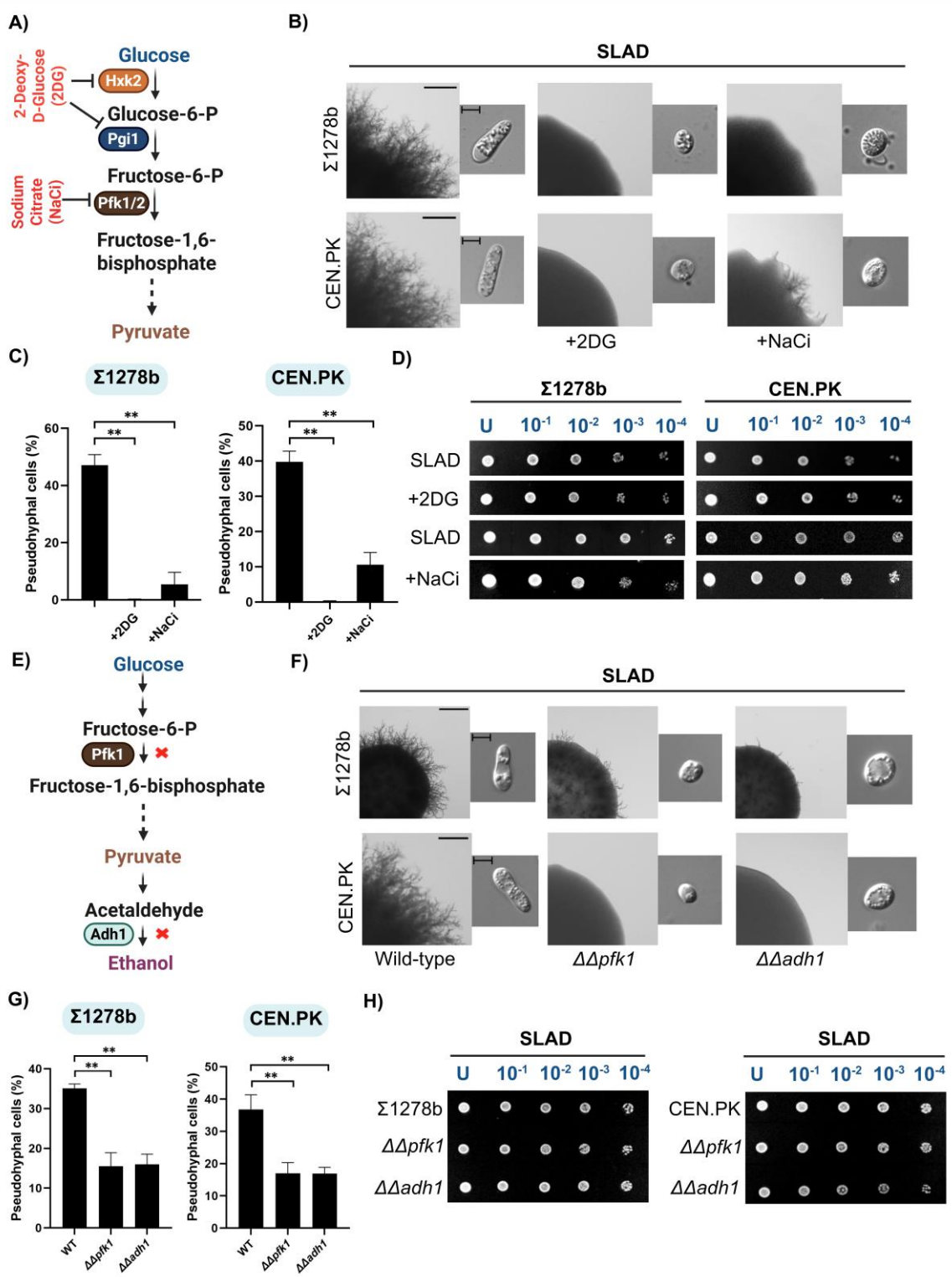

Fig 2. Ability of Cells to Metabolize glucose *via* glycolysis is critical for Fungal Morphogenesis

(A) Schematic overview of glycolysis and its inhibition by glycolysis inhibitors (2-Deoxy-D-Glucose (2DG) and sodium citrate (NaCi)). **(B)** Wild-type Σ1278b or CEN.PK were spotted on nitrogen-limiting medium containing 2% glucose (SLAD) with and without sub-inhibitory concentrations of glycolysis inhibitors (2-Deoxy-D-Glucose (2DG) and sodium citrate (NaCi)), incubated for 10 days at 30 °C. Whole colony imaging was done using Olympus MVX10 stereo microscope and single cell

1203 imaging was done using Zeiss Apotome microscope. Scale bar represents 1mm for whole colony
1204 images and 5μm for single cell images. **(C)** Cells from colonies were isolated and single cells were
1205 imaged using Zeiss Apotome microscope and percentage of pseudohyphal cells were calculated using
1206 ImageJ. Statistical analysis was done using unpaired t-test, **(P<0.01). Error bars represent SEM.
1207 **(D)** Spot dilution assay was performed to monitor overall growth of wild-type strains on SLAD,
1208 SLAD+2DG and SLAD+NaCi with the following serial dilutions (U-Undiluted, 10^{-1}-1:10 dilution,
1209 10^{-2}-1:100 dilution, 10^{-3}-1:1000 dilution, 10^{-4}-1:10000 dilution). **(E)** Schematic overview of
1210 glycolysis showing targeted gene deletions. **(F)** Pertinent knockout strains which lack genes
1211 encoding for enzymes involved in glycolysis such as *pfk1* and *adh1* were spotted on SLAD along with
1212 wild-type ∑1278b or CEN.PK. Whole colony imaging was done using Olympus MVX10 stereo
1213 microscope and single cell imaging was done using Zeiss Apotome microscope. Scale bar represents
1214 1mm for whole colony images and 5μm for single cell images. **(G)** Cells from colonies were isolated
1215 and single cells were imaged using Zeiss Apotome microscope and percentage of pseudohyphal cells
1216 were calculated using ImageJ. Statistical analysis was done using unpaired t-test, **(P<0.01). Error
1217 bars represent SEM. **(H)** Spot dilution assay was performed to monitor overall growth of wild-type
1218 and knockout strains on SLAD with the following serial dilutions (U-Undiluted, 10^{-1}-1:10 dilution, 10^{-}
1219 ^{2}-1:100 dilution, 10^{-3}-1:1000 dilution, 10^{-4}-1:10000 dilution).

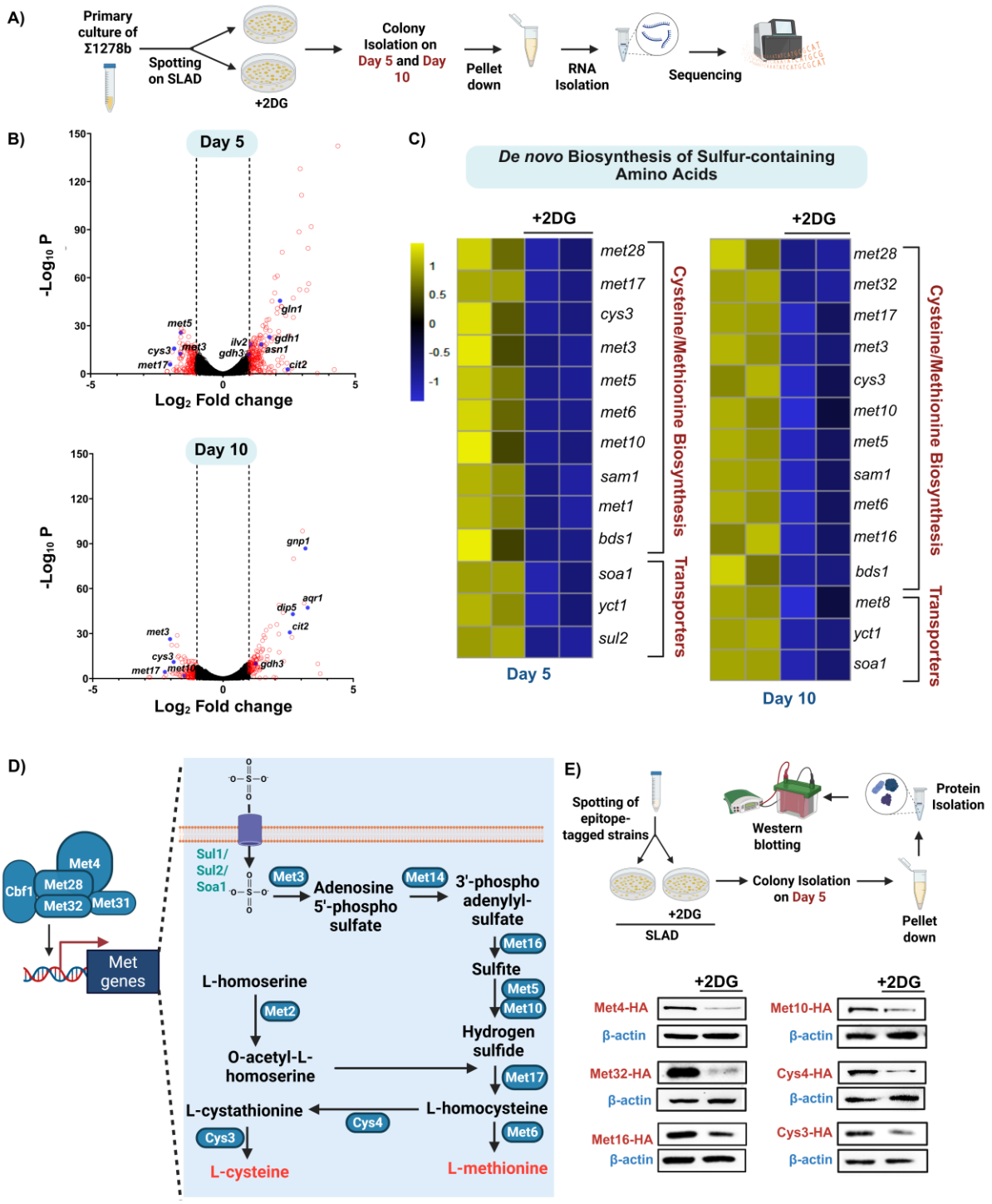

Fig 3. Comparative Transcriptomics Identifies the Role of Glycolysis in Regulating Sulfur Metabolism During Fungal Morphogenesis

(A) Schematic overview of steps involved in RNA isolation and RNA-sequencing. **(B)** Volcano plots represent differentially expressed genes in 2DG treated cells compared to untreated cells isolated from D-5 and D-10 colonies, respectively. Genes which are upregulated (Log_2 fold change ≥ 1) and downregulated (Log_2 fold change ≤ -1) are highlighted in red. Some of the significantly upregulated and downregulated genes involved in the biosynthesis of various amino acids are highlighted in blue. **(C)** Heatmaps represent differential expression of individual genes involved in *de novo* biosynthesis and transport of sulfur-containing amino acids, in 2DG treated cells compared to untreated cells

1231 isolated from D-5 and D-10 colonies, respectively. **(D)** Schematic overview of *de novo* biosynthesis
1232 of sulfur-containing amino acids. **(E)** Schematic overview of steps involved in the Western blotting
1233 experiments. Epitope-tagged strains of various proteins involved in the *de novo* biosynthesis of
1234 sulfur-containing amino acids including Met4p, Met32p, Met16p, Met10p, Cys4p and Cys3p were
1235 spotted on SLAD in the presence and absence of sub-inhibitory concentration of 2DG following which,
1236 cells from colonies were isolated on D-5 and levels of these proteins were assessed using Western
1237 blotting. β-actin was used as loading control.
1238

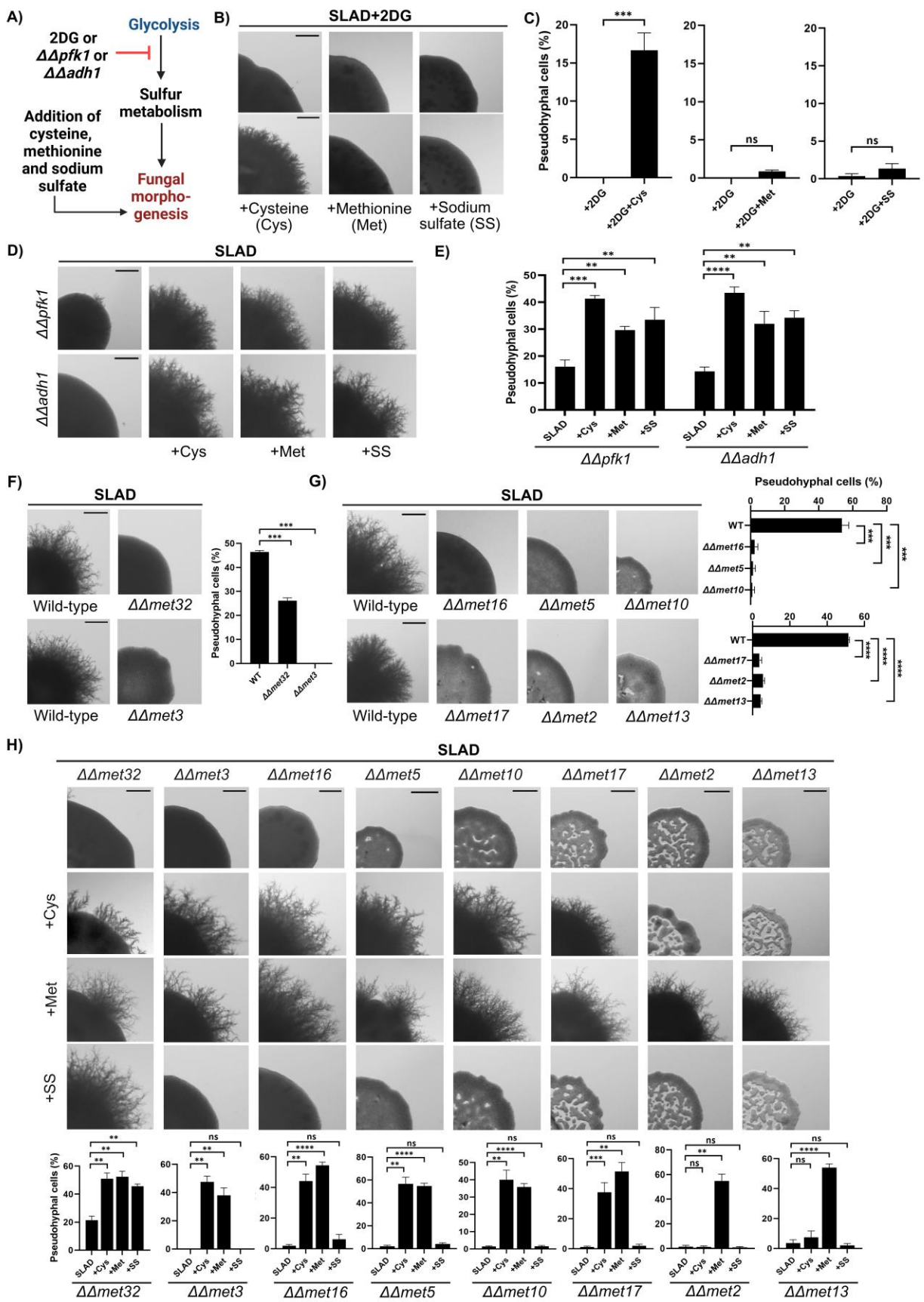
A)
Glycolysis
2DG or
ΔΔpfk1 or
ΔΔadh1
Sulfur metabolism
Addition of cysteine, methionine and sodium sulfate
Fungal morpho-genesis
B)
SLAD+2DG
+Cysteine (Cys)
+Methionine (Met)
+Sodium sulfate (SS)
C)
Pseudohyphal cells (%)
+2DG
+2DG+Cys
+2DG+Met
+2DG+SS
ns
D)
SLAD
ΔΔpfk1
ΔΔadh1
+Cys
+Met
+SS
E)
Pseudohyphal cells (%)
SLAD
+Cys
+Met
+SS
ΔΔpfk1
ΔΔadh1
F)
SLAD
Wild-type
ΔΔmet32
ΔΔmet3
WT
G)
SLAD
Wild-type
ΔΔmet16
ΔΔmet5
ΔΔmet10
ΔΔmet17
ΔΔmet2
ΔΔmet13
H)
SLAD
ΔΔmet32
ΔΔmet3
ΔΔmet16
ΔΔmet5
ΔΔmet10
ΔΔmet17
ΔΔmet2
ΔΔmet13
+Cys
+Met
+SS

1239

1240

1241 **Fig 4. Glycolysis-mediated Regulation of Sulfur Metabolism is Critical for Fungal**
1242 **Morphogenesis**

1243 **(A)** Schematic overview of the proposed role of glycolysis-dependent sulfur metabolism in regulating
1244 pseudohyphal differentiation under nitrogen-limiting conditions in *S. cerevisiae.* **(B)** Wild-type
1245 ∑1278b was spotted on SLAD containing sub-inhibitory concentration of 2DG with and without sulfur-
1246 containing compounds including cysteine (500μM), methionine (20μM) or sodium sulfate (1000μM),
1247 incubated for 10 days at 30 °C. After 10 days, whole colony imaging was done using Olympus MVX10
1248 stereo microscope. Scale bar represents 1mm for whole colony images. **(C)** Cells from colonies were
1249 isolated and single cells were imaged using Zeiss Apotome microscope and percentage of
1250 pseudohyphal cells were calculated using ImageJ. Statistical analysis was done using unpaired
1251 t-test, ***(P<0.001) and ns (non-significant). Error bars represent SEM. **(D)** Pertinent knockout
1252 strains which lack genes encoding for enzymes involved in glycolysis such as *pfk1* and *adh1* were
1253 spotted on SLAD with and without sulfur-containing compounds including cysteine (200μM),
1254 methionine (20μM) or sodium sulfate (1000μM), incubated for 10 days at 30 °C. After 10 days,
1255 whole colony imaging was done using Olympus MVX10 stereo microscope. Scale bar represents 1mm
1256 for whole colony images. **(E)** Cells from colonies were isolated and single cells were imaged using
1257 Zeiss Apotome microscope and percentage of pseudohyphal cells were calculated using ImageJ.
1258 Statistical analysis was done using unpaired t-test, ****(P<0.0001), ***(P<0.001) and
1259 **(P<0.01). Error bars represent SEM. **(F)** Pertinent knockout strains which lack genes encoding
1260 for enzymes involved in *de novo* biosynthesis of sulfur-containing amino acids including *met32* and
1261 *met3* along with wild-type ∑1278b were spotted on SLAD and imaged after 10 days using Olympus
1262 MVX10 stereo microscope. Scale bar represents 1mm for whole colony images. Cells from colonies
1263 were isolated and single cells were imaged using Zeiss Apotome microscope and percentage of
1264 pseudohyphal cells were calculated using ImageJ. Statistical analysis was done using unpaired
1265 t-test, ***(P<0.001). Error bars represent SEM. **(G)** Pertinent knockout strains which lack genes
1266 involved in *de novo* biosynthesis of sulfur-containing amino acids such as *met16*, *met5*, *met10*,
1267 *met17*, *met2* and *met13* along with wild-type ∑1278b were spotted on SLAD and imaged after 10
1268 days using Olympus MVX10 stereo microscope. Scale bar represents 1mm for whole colony images.
1269 Cells from colonies were isolated and single cells were imaged using Zeiss Apotome microscope and
1270 percentage of pseudohyphal cells were calculated using ImageJ. Statistical analysis was done using
1271 unpaired t-test, ****(P<0.0001) and ***(P<0.001). Error bars represent SEM. **(H)** Pertinent
1272 knockout strains including *ΔΔmet32*, *ΔΔmet3, ΔΔmet16, ΔΔmet5, ΔΔmet10, ΔΔmet17, ΔΔmet2* and
1273 *ΔΔmet13* were spotted on SLAD with and without sulfur-containing compounds including cysteine
1274 (200μM), methionine (20μM) or sodium sulfate (1000μM), incubated for 10 days at 30 °C. After 10
1275 days, imaging was done using Olympus MVX10 stereo microscope. Scale bar represents 1mm for
1276 whole colony images. Cells from colonies were isolated and single cells were imaged using Zeiss
1277 Apotome microscope and percentage of pseudohyphal cells were calculated using ImageJ. Statistical
1278 analysis was done using unpaired t-test, ****(P<0.0001), ***(P<0.001), **(P<0.01) and ns (non-
1279 significant). Error bars represent SEM.
1280

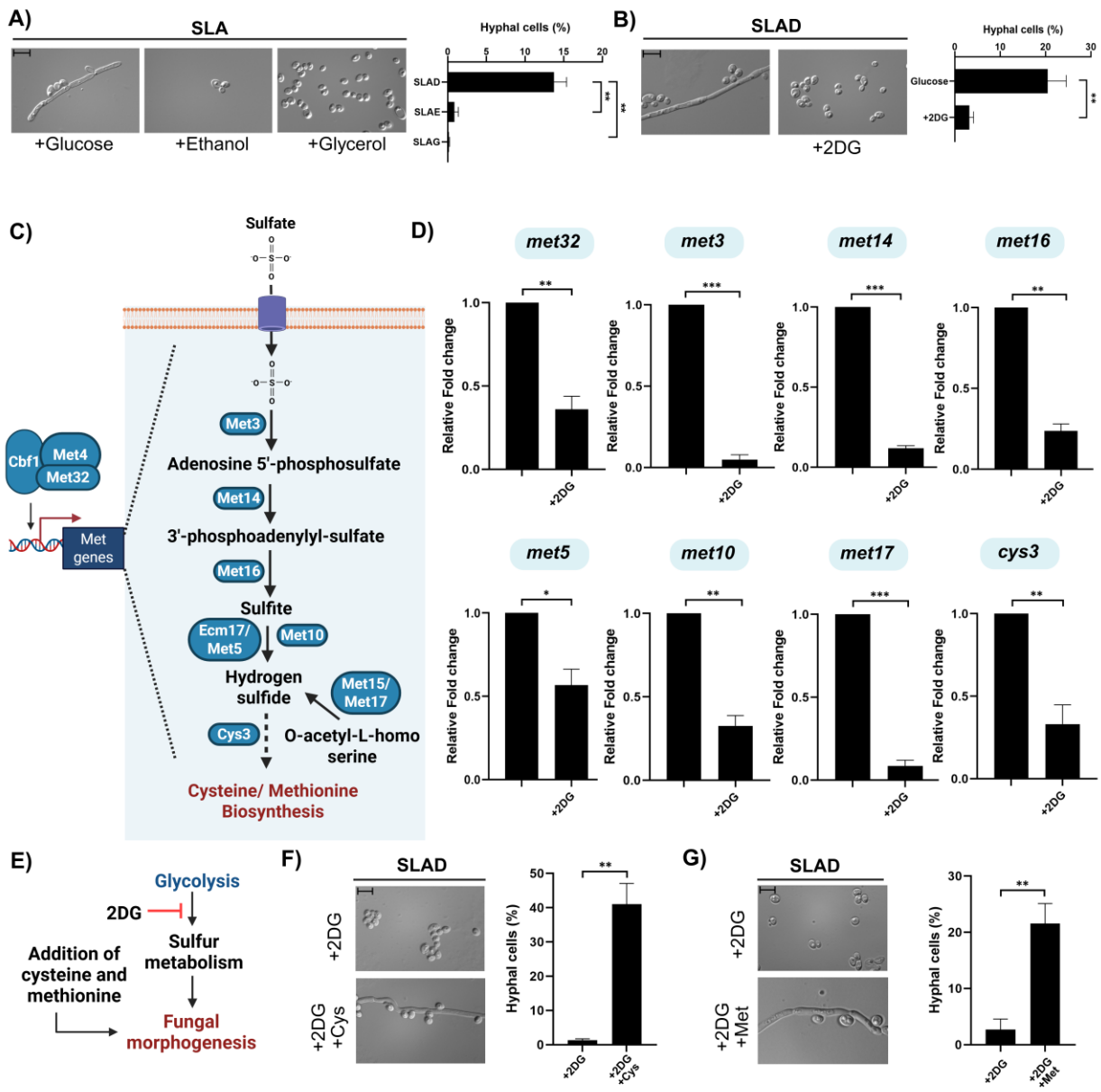

Fig 5. Glycolysis-dependent Sulfur Metabolism is Critical for Fungal Morphogenesis in *Candida albicans*

(A) Wild-type SC5314 was spotted on SLAD and SLA containing non-fermentative carbon sources including ethanol and glycerol (2%), incubated for 7 days at 37 °C. Cells from colonies were isolated and single cells were imaged using Zeiss Apotome microscope and percentage of hyphal cells were calculated using ImageJ. Scale bar represents 10µm for single cell images. Statistical analysis was done using unpaired t-test, **(P<0.01). Error bars represent SEM. **(B)** Wild-type SC5314 was spotted on SLAD with and without sub-inhibitory concentration of glycolysis inhibitor 2DG, incubated for 7 days at 37 °C. Cells from colonies were isolated and single cells were imaged using Zeiss Apotome microscope and percentage of hyphal cells were calculated using ImageJ. Scale bar represents 10µm for single cell images. Statistical analysis was done using unpaired t-test, **(P<0.01). Error bars represent SEM. **(C)** Schematic overview of *de novo* biosynthesis of sulfur-containing amino acids. **(D)** Wild-type SC5314 was spotted on SLAD, in the presence and absence of sub-inhibitory concentration of 2DG and cells from colonies were isolated after ~4 days, for RNA isolation. We then performed comparative RT-qPCR to check for the relative expression of genes involved in the *de novo* biosynthesis of sulfur-containing amino acids pathway including *met32*,

met3, *met14*, *met16*, *met5*, *met10*, *met17* and *cys3.* Statistical analysis was done using unpaired t-test, ***(P<0.001), **(P<0.01) and *(P<0.05). Error bars represent SEM. **(E)** Schematic overview of the proposed role of glycolysis-dependent sulfur metabolism in regulating hyphal differentiation under nitrogen-limiting conditions in *C. albicans*. **(F)** Wild-type SC5314 was spotted on SLAD containing sub-inhibitory concentration of 2DG with and without cysteine (100μM) and, incubated for 7 days at 37 °C. Cells from colonies were isolated and single cells were imaged using Zeiss Apotome microscope and percentage of hyphal cells were calculated using ImageJ. Scale bar represents 10μm for single cell images. Statistical analysis was done using unpaired t-test, **(P<0.01). Error bars represent SEM. **(G)** Wild-type SC5314 was spotted on SLAD containing sub-inhibitory concentration of 2DG with and without methionine (20μM) and, incubated for 7 days at 37 °C. Cells from colonies were isolated and single cells were imaged using Zeiss Apotome microscope and percentage of hyphal cells were calculated using ImageJ. Scale bar represents 10μm for single cell images. Statistical analysis was done using unpaired t-test, **(P<0.01). Error bars represent SEM.

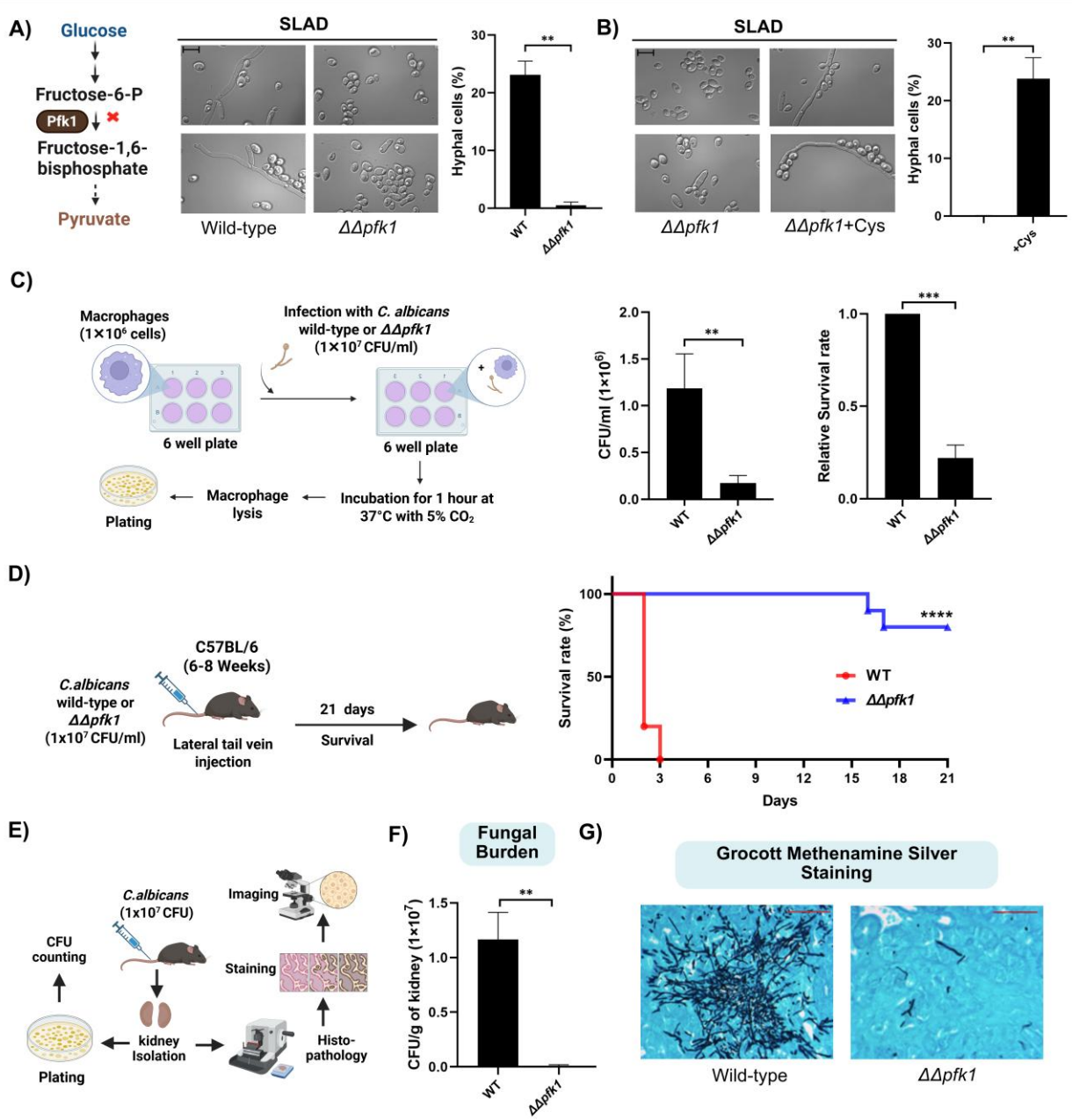

Fig 6._Perturbation of Glycolysis Leads to Attenuated Fungal Virulence

(A) Schematic overview of glycolysis showing targeted gene deletion of *pfk1*. Wild-type SC5314 and pertinent knockout strain which lacks the genes encoding for a glycolytic enzyme, *pfk1* (*ΔΔpfk1*) were spotted on SLAD, incubated for 7 days at 37 °C. Cells from colonies were isolated and single cells were imaged using Zeiss Apotome microscope (2 representative images are shown for each strain) and percentage of hyphal cells were calculated using ImageJ. Scale bar represents 10μm for single cell images. Statistical analysis was done using unpaired t-test, **(P<0.01). Error bars represent SEM. **(B)** *ΔΔpfk1* was spotted on SLAD in the presence and absence of cysteine (100μM), incubated for 7 days at 37 °C. Cells from colonies were isolated and single cells were imaged using Zeiss Apotome microscope (2 representative images are shown for each condition) and percentage of hyphal cells were calculated using ImageJ. Statistical analysis was done using unpaired t-test, **(P<0.01). Error bars represent SEM. **(C)** Schematic overview of *ex vivo* microbial survival assay. *RAW 264.7* macrophages were incubated with the wild-type and *ΔΔpfk1* strain with MOI=10. After 1 hour of incubation, macrophages were lysed and plating was done to enumerate CFU. Percentage of survival was expressed as the number of CFUs in the presence of macrophages divided by the

number of CFUs in the absence of macrophages. Statistical analysis was done using unpaired t-test, **(P<0.01). Error bars represent SEM. **(D)** 6- 8-week-old C57BL/6 mice were infected intravenously *via* lateral tail vein injection with 1×10^7 CFU/ml of wild-type SC5314 or 1×10^7 CFU/ml of *ΔΔpfk1*. To determine survival rate, mice were monitored for 21 days post-infection for clinical signs of illness or mortality. The results are representative of ten mice per injected strain. Survival percentage were statistically evaluated by the Log-rank Mantel-Cox test, ****(P=0.0001) (n=10). **(E)** Schematic overview of kidney isolation to check fungal burden using CFU counting and histology. **(F)** Fungal burden was measured by CFU counting after kidney isolation from mice injected with either wild-type or *ΔΔpfk1*. Statistical analysis was done using unpaired t-test, *(P<0.05). Error bars represent SEM. **(G)** Histopathological analysis of kidney sections using Grocott Methanamine Silver (GMS) staining was done for kidneys isolated from mice injected with either wild-type SC5314 or *ΔΔpfk1*. Fungal cells appear black in colour against the colored background of the kidney tissue. Bright field imaging was done using Axioplan 2 microscope at 40X magnification. Scale bar represents 50 μm.

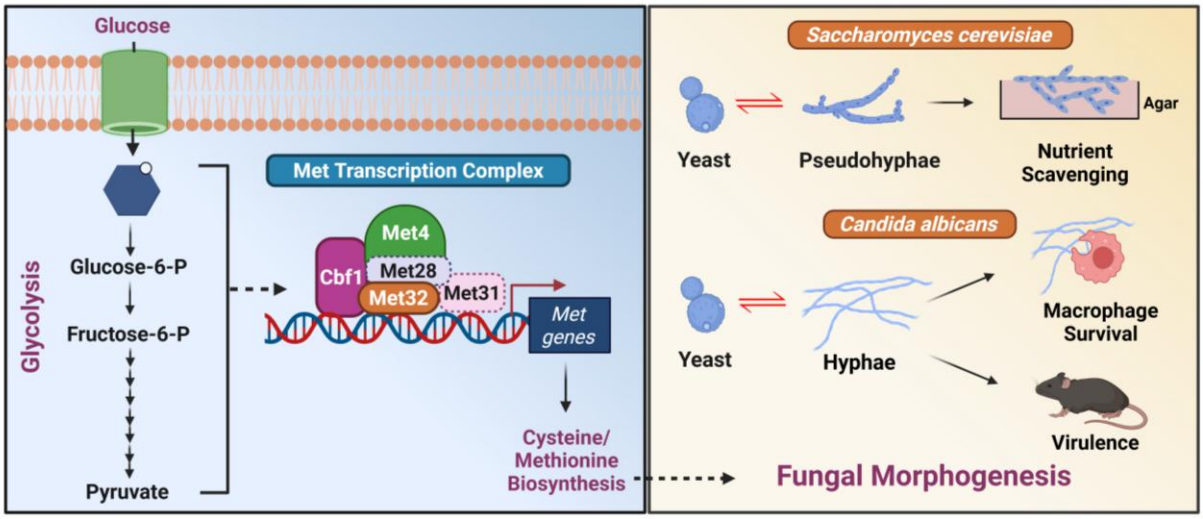

Fig 7. Glycolysis-dependent Sulfur Metabolism Orchestrates Morphological Transitions and Virulence in Fungi

Active glycolysis plays a key regulatory role in the *de novo* biosynthesis of sulfur-containing amino acids by modulating the expression of genes involved in this process (In *S. cerevisiae*, Met transcription complex includes Met4p, Met28p, Cbf1p, Met31p, and Met32p, whereas in *C. albicans*, the characterized components of this complex include Met4p, Cbf1p, and Met32p. Hence, Met28p and Met31p, unique to the Met transcription complex of *S. cerevisiae* are represented with dotted borders). Glycolysis-dependent sulfur metabolism in turn, is critical for fungal morphogenesis in both species and the ability of *C. albicans* to survive within macrophages and cause systemic infection in a *murine* model of candidiasis.

Supporting Information

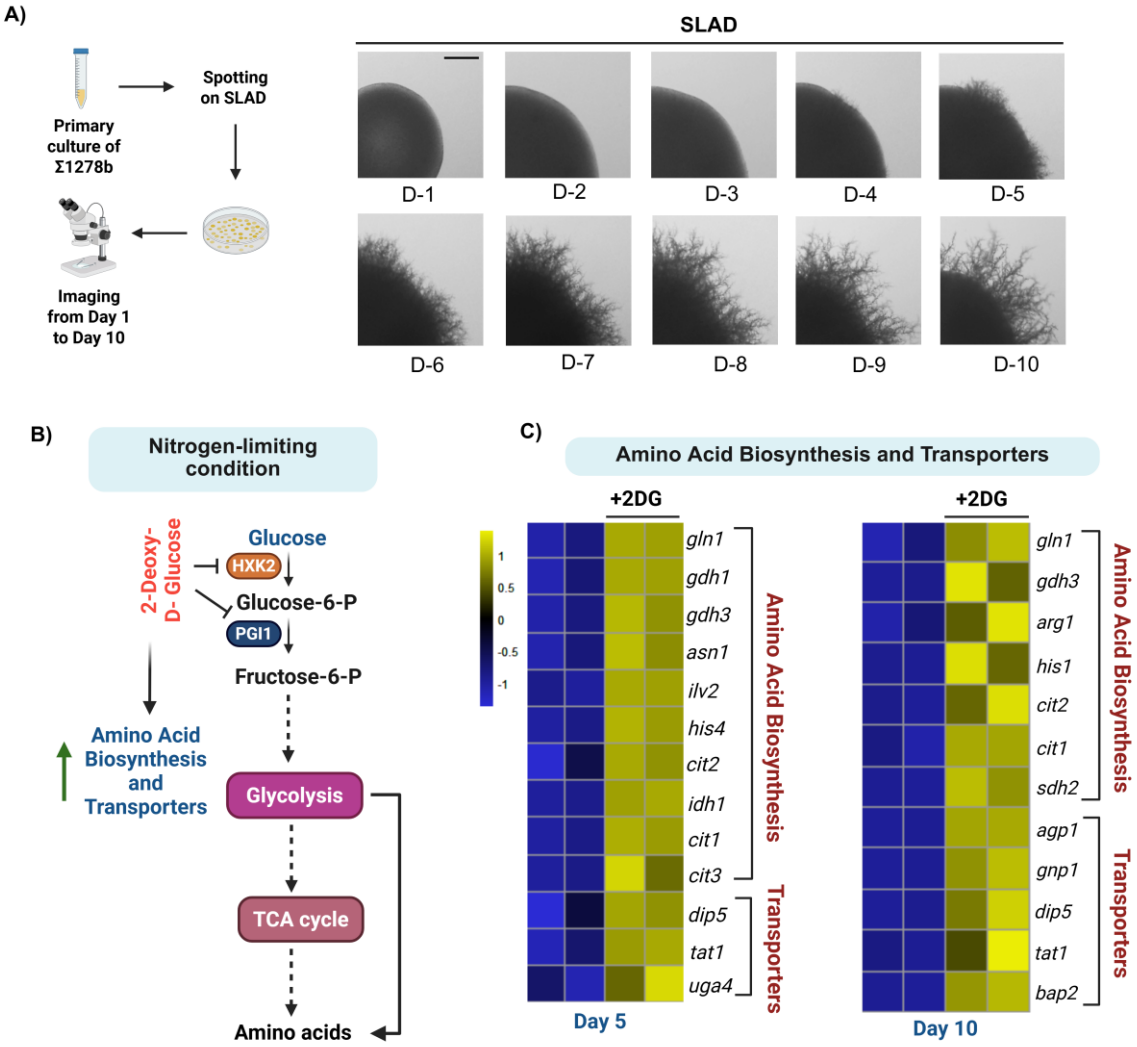

S1 Fig. Comparative Transcriptomics Identifies the Transcriptional Landscape of Cells Undergoing Pseudohyphal Differentiation

(A) Wild-type ∑1278b was spotted on SLAD, incubated for 10 days at 30 °C. Colonies were imaged every day, for 10 consecutive days (D-1 to D-10), using Olympus MVX10 stereo microscope. Scale bar represents 1mm for whole colony images. **(B)** Schematic overview of the regulation of amino acid biosynthesis under nitrogen-limiting condition. **(C)** Heatmaps represent differential expression of individual genes involved in biosynthesis and transport of various amino acids, in 2DG treated cells compared to untreated cells isolated from day 5 and day 10 colonies, respectively.

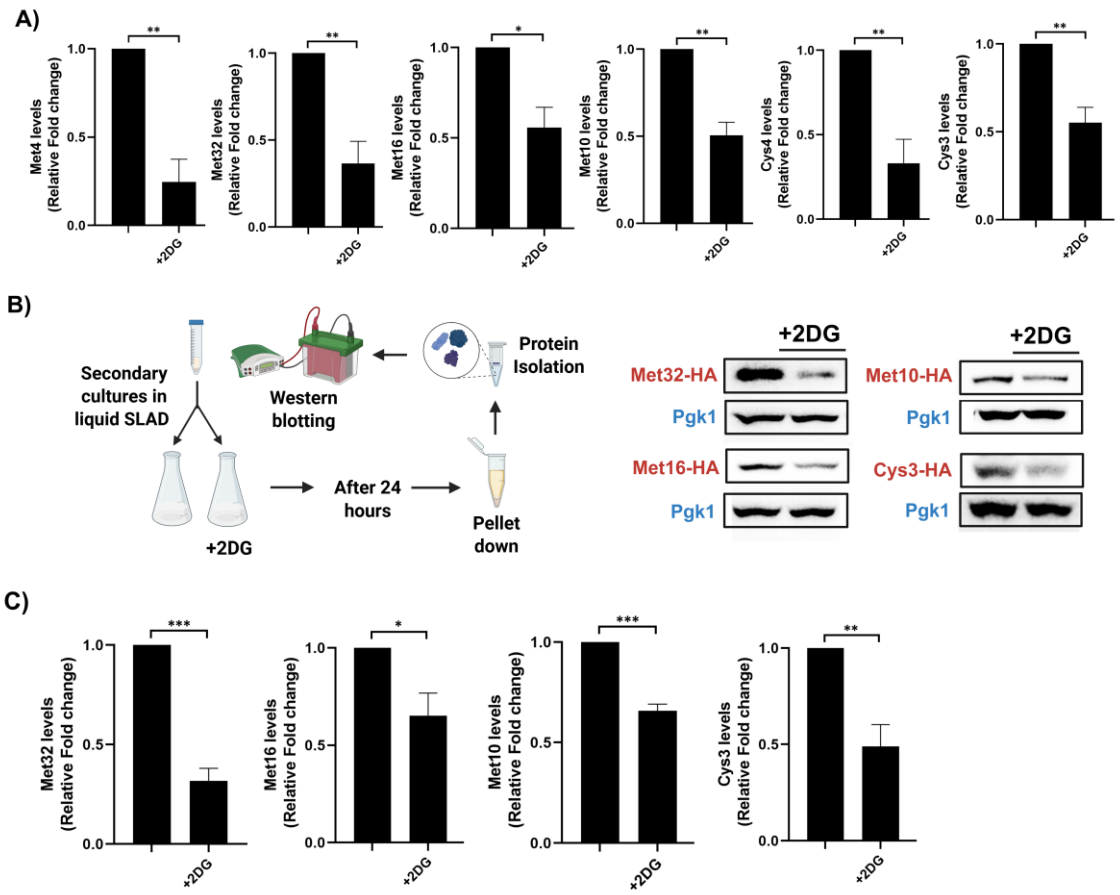

S2 Fig. Expression of Proteins Involved in the *de novo* Biosynthesis of Sulfur-containing Amino Acids in Response to Glycolysis Perturbation

(A) Epitope-tagged strains of various proteins involved in the *de novo* biosynthesis of sulfur-containing amino acids including Met4p, Met32p, Met16p, Met10p, Cys4p and Cys3p were spotted on SLAD in the presence and absence of sub-inhibitory concentration of 2DG following which, cells from colonies were isolated at day 5 and levels of these proteins were assessed using Western blotting. Raw images of western blots were analysed using ImageJ to normalize targeted protein expression with the expression of housekeeping protein- β-actin, in order to generate densitometric graphs. Statistical analysis was done using unpaired t-test, **(P<0.01) and *(P<0.05). Error bars represent SEM. **(B)** Epitope-tagged strains of various proteins involved in the *de novo* biosynthesis of sulfur-containing amino acids including Met32p, Met16p, Met10p and Cys3p were grown in liquid SLAD and then treated with sub-inhibitory concentration of 2DG for 24 hours after which protein expression was checked using Western blotting. Pgk1p was used as loading control. **(C)** Raw images of western blots were analysed using ImageJ to normalize targeted protein expression with the expression of housekeeping protein- Pgk1p, in order to generate densitometric graphs. Statistical analysis was done using unpaired t-test, ***(P<0.001), **(P<0.01) and *(P<0.05). Error bars represent SEM.

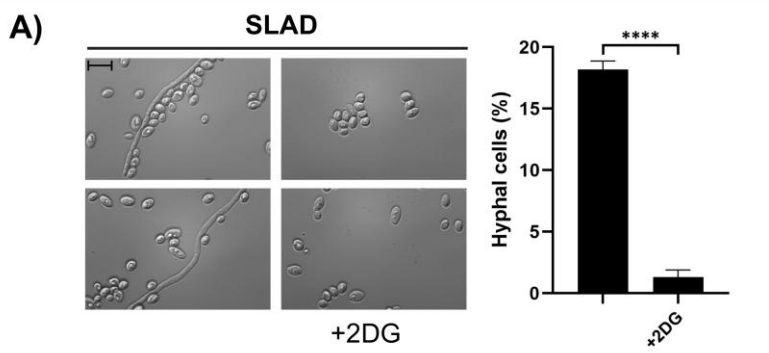

S3 Fig. *C. albicans* Hyphal Differentiation Assay

(A) Wild-type SC5314 was spotted on SLAD with and without sub-inhibitory concentration of 2DG, incubated for ~4 days at 37 °C. Cells from colonies were isolated and single cells were imaged using Zeiss Apotome microscope (2 representative images are shown for each condition) and percentage of hyphal cells were calculated using ImageJ. Scale bar represents 10μm for single cell images. Statistical analysis was done using unpaired t-test, ****($P<0.0001$). Error bars represent SEM.

1513 **S1 Table. Yeast Strains Used in this Study**

Strain	Genotype
***S. cerevisiae* Σ1278b**	
Wild-type	*MATa/α*
SV18	*Δadh1::G418/Δadh1::HygB MATa/α*
SV21	*Δpfk1::HygB/Δpfk1::G418 MATa/α*
SV270	*Δmet32::NAT/Δmet32::G418 MATa/α*
SV281	*Δmet2::NAT/Δmet2::G418 MATa/α*
SV299	*Δmet17::NAT/Δmet17::G418 MATa/α*
SV305	*Δmet13::G418/Δmet13::NAT MATa/α*
SV311	*Δmet3::NAT/Δmet3::G418 MATa/α*
SV320	*MET32-HA::G418/MET32-HA::NAT MATa/α*
SV350	*Δmet5::NAT/Δmet5::G418 MATa/α*
SV386	*Δmet10::NAT/Δmet10::G418 MATa/α*
SV388	*Δmet16::NAT/Δmet16::G418 MATa/α*
SV394	*CYS3-HA::NAT/CYS3-HA::G418 MATa/α*
SV395	*CYS4-HA::NAT/CYS4-HA::G418 MATa/α*
SV402	*MET10-HA::NAT/MET10-HA::G418 MATa/α*
SV404	*MET16-HA::NAT/MET16-HA::G418 MATa/α*
SV461	*MET4-HA::NAT/MET4-HA::G418 MATa/α*
***S. cerevisiae* CEN.PK**	
Wild-type	*MATa/α*
SV109	*Δadh1::G418/Δadh1::NAT MATa/α*
SV117	*Δpfk1::NAT/Δpfk1::G418 MATa/α*
***C. albicans* SC5314**	
Wild-type	*MATa/α*
SV308	*Δpfk1::FRT/Δpfk1::SAT-FLP MATa/α*

1514

1515

1516 **S2 Table. Oligonucleotides Used in this Study**

Oligonucleotides	Sequence (5′ to 3′)
Primers for *S. cerevisiae* Gene Editing and Genotyping	
ADH1 KO F1	AGCTATACCAAGCATACAATCAACTATCTCATATACAATGCGGATCCCCGGGTTAATTAA
ADH1 R1	ATTTAATAATAAAAATCATAAATCATAAGAAATTCGCTTAGAATTCGAGCTCGTTTAAAC
ADH1 KO Chk	CGTTGTTGTCTCACCATATC
PFK1 KO F1	TTTTATATAAAAAATCTGAAACAAAATCATATCAAAGATGCGGATCCCCGGGTTAATTAA
PFK1 R1	CTCCTTTTGCTTAACTTAAACTTTTCATTGCAATCATTCAGAATTCGAGCTCGTTTAAAC
PFK1 KO Chk	AGGATGAGAAAGTGAAATCG
MET32 KO F1	AAGTCAAGAGGTATTATAAATTTCAAAAAAGTACCAAATGCGGATCCCCGGGTTAATTAA

MET32 R1	ATTTTCTTATTTGAGAAGATACACGCTATTTACTCTTTCAGAATTCGAGCTCGTTTAAAC
MET32 KO Chk	GATGGTTTTTCGTCCCTTAC
MET17 KO F1	GATACATAGATACAATTCTATTACCCCCATCCATACAATGCGGATCCCCGGGTTAATTAA
MET17 R1	TAGGTTTATACATAATTTTACAACTCATTACGCACACTCAGAATTCGAGCTCGTTTAAAC
MET17 KO Chk	TTTTGCTTTTTCTCTTGAGG
MET13 KO F1	AGAACCACCACAGTTACTACTACAACCACATCGCAATATGCGGATCCCCGGGTTAATTAA
MET13 R1	CAATTCTGTTAAAGAACTGTTATCGTTGTCTGTGTTATTAGAATTCGAGCTCGTTTAAAC
MET13 KO Chk	AGGAAAAGTTGGCGATAGAC
MET3 KO F1	GAAAGTATAATAATAACAAGAATAAAGTATAATTAACATGCGGATCCCCGGGTTAATTAA
MET3 R1	TTTGCCCTACTTTTGAGATGGGAGCATTTTATGACGATTAGAATTCGAGCTCGTTTAAAC
MET3 KO Chk	CACGTGACCAGAAAAGTCAC
MET2 KO F1	TAATAGAAAAGAAAGAAAAAAACGTAGTATAAAAGGAATGCGGATCCCCGGGTTAATTAA
MET2 R1	ATCTATGTTATGCCTGAGGTATGTGTGGTATCTATCCCTAGAATTCGAGCTCGTTTAAAC
MET2 KO Chk	TTCAGTTTGTCAAGGTTATGC
MET32 C tag F1	TCATCGTCAAGATAACAACCACAATGGTAGCAGTAATGGCCGGATCCCCGGGTTAATTAA
MET32 C tag Chk	GATGGTTTTTCGTCCCTTAC
CYS3 C tag F1	TTTGGAAGACATCAAGCAAGCCTTGAAACAAGCCACCAACCGGATCCCCGGGTTAATTAA
CYS3 R1	AAAGGTCCGGTCGAAGGCAGAGACGTGGCACTGGCGATTAGAATTCGAGCTCGTTTAAAC
CYS3 C tag Chk	CAGAGGTTTGAAGACTTTGC
Met10 Ctag F1	AGAATTAAAGGAAGCATCAAGATACATTTTAGAAGTCTACCGGATCCCCGGGTTAATTAA
Met10 Ctag Chk	TGGTTTAGGTACTGGTTTGG
Met16 Ctag F1	TGAAGCCAGCCGATTCGCGCAATTTTTAAAGCAAGATGCCCGGATCCCCGGGTTAATTAA
Met16 Ctag Chk	AATACGGGGATTTCTTATGG
Met4 Ctag F1	AAGCTTAAAGAAGCAAATTTTTGAGAAGGTTCAGAAAGAACGGATCCCCGGGTTAATTAA
Met4 R1	TATATATATATATAATTAAACTGTATAGTCTGTTATTTTAGAATTCGAGCTCGTTTAAAC
Met4 Ctag Chk	GAGCCAACTTTAAATGCAAG
Cys4 Ctag F1	CCATATCGTTACTAAGATGGATTTACTGAGCTACTTAGCACGGATCCCCGGGTTAATTAA
Cys4 R1	TTCTATGTTTGCTTTTATTTGAAGCGTGGGTTCTTATTTAGAATTCGAGCTCGTTTAAAC
Cys4 Ctag Chk	TTAAGGAAACCGCTAAGGTC

Primers for *C. albicans* Gene Editing and Genotyping	
Psfs2a PFK1 F1	ATTTGAATAGCTTTTTCTTATTATTGAATTCTTTAATTTATCGTTTATTGCAAACA ATCAATTATTCCTTATTATTTTGGGCAGATAACGAATTAGAAATGAAGTTCCTAT ACTTTCTAG
Psfs2a PFK1 R1	CAACACATTGAATTACATATATGAGTATAAAAAATCAAACTATACTGGGGACTA CAAATCTTACTATTTTACACAACTCCTTATCTTCTGTTCTTCATTTGAAGTTCCTA TTCTCTAGAA
Psfs2a SAT-FLP F1	AACATTGGATGCTGAGAACC
Psfs2a SAT-FLP R1	GCACATAATGCTATTTTCTC
PFK1 ApaI UF1	GAGAGGGCCCGTGATGCCTAACTTCTTGGT
PFK1 SacII DR1	CTCTCCGCGGTAGGCTGAATTGCTCGTATG
Pfk1 KO R1 Chk	GTACCAATTGAAGTACCACC
FRT F1	CTTTCTAGAGAATAGGAACT
FRT R1	AGTTCCTATTCTCTAGAAAG
Primers for RT-qPCR	
Candida Act1 F1	TTGGATTCTGGTGATGGTGTTA
Candida Act1 R1	TCAAGTCTCTACCAGCCAAATC
Candida Met32 F1	CACCAACACAACACCATCAAC
Candida Met32 R1	TCCAATTCCACCACCAGTAATC
Candida Met3 F1	GTTCCAACAACAAACCCAACTC
Candida Met3 R1	TCACCATCAGCATTACCAGAAG
Candida Met14 F1	GTTGCTGAACAAAGAGATCCAAA
Candida Met14 R1	CCTGAATGGTTCTTAACGTGTATTT
Candida Met16 F1	GAGTTTCGGCTGTGCTAACT
Candida Met16 R1	TTCCACTTGTTTCCTCGTATTCT
Candida Met5 F1	TTTATGGTGCGTGTTCGTTTAC
Candida Met5 R1	TAGCCCTGGTGGTCAATTTC
Candida Met10 F1	GGGTTGATCCAAAGGGAAGAT
Candida Met10 R1	GACAATGGTGGCAACTTCATAAC
Candida Met17 F1	TCAAGGACATCACCAACACC
Candida Met17 R1	CTTAGAGTCACCCACATTAGCC
Candida Cys3 F1	TCGCCATACCTTTCCAATCC
Candida Cys3 R1	GGTTGCCAAGACTCCCATAA

1517

1518 **S3 Table. List of Reagents and Tools Used in this Study**

Reagents/ Resource	**Reference or Source**	**Identifier or catalog Number**
Recombinant DNA		
pFA6a-kanMX	Gift from Dr. Sunil Laxman	Not applicable
pFA6a-Hyg	Gift from Dr. Sunil Laxman	Not applicable
pFA6a-Nat	Gift from Dr. Sunil Laxman	Not applicable
pFA6a-Ctag-HA-G418	Gift from Dr. Sunil Laxman	Not applicable
pFA6a-Ctag-HA-NAT	Gift from Dr. Sunil Laxman	Not applicable

pSFS2a-NAT	Gift from Dr. Kaustuv Sanyal	Not applicable
Antibodies		
Rabbit anti-HA	Cell Signaling Technology	3724S
Mouse anti-β-actin	Cell Signaling Technology	3700
Mouse anti-PGK1	Santa Cruz Biotechnology	sc-130335
Goat anti-Rabbit IgG-HRP conjugate	Cell Signaling Technology	7074S
Horse anti-Mouse IgG-HRP conjugate	Cell Signaling Technology	7076S
Chemicals, enzymes and other reagents		
BD Bacto agar	Becton Dickinson	214010
Agarose	MP Biomedicals	100267
Ammonium sulfate	Sisco Research Laboratories	0149175
Blotto, non-fat dry milk	Santa Cruz Biotechnology	sc-2324
B-mercaptoethanol	Sigma-Aldrich	444203
Diluent	HiMedia	MB228
D-(+)-Glucose anhydrous	HiMedia	GRM016
Lithium acetate	Sigma-Aldrich	517992
Peptone	Thermo Fisher Scientific	211677
RNaseZAP	Sigma-Aldrich	R2020
SDS	G Biosciences	RC1184
Trichloro acetic acid	Sigma-Aldrich	100807
Tris, free base	HiMedia	MB029
Tween 20	Sigma-Aldrich	P7949
Yeast extract	Thermo Fisher Scientific	212750
Yeast nitrogen base w/o amino acids and ammonium sulfate	Becton Dickinson	233520
D-Sucrose	HiMedia	GRM3063
D-Fructose	Sigma-Aldrich	F3510
D-Maltose	Sigma-Aldrich	M5895
D-Mannose	Sigma-Aldrich	63580
D-Trehalose	Sigma-Aldrich	T0167
D-Galactose	Sigma-Aldrich	48260
L-Cysteine	Sigma-Aldrich	30089
L-Methionine	Sigma-Aldrich	64319
DL-Glyceraldehyde	Sigma-Aldrich	G5001
Sodium citrate	Sigma-Aldrich	C8532
Sodium sulfate	HiMedia	GRM1037
Glycerol	HiMedia	MB060
Potassium acetate	MP Biomedicals	191425
2-Deoxy-D-Glucose	Sigma-Aldrich	D8375
NAT	Jena Bioscience	AB-102XL
G418	MP Biomedicals	158782
Ethidium bromide	HiMedia	MB074
Pico-ECL substrate	Thermo Fisher Scientific	34579
Femto-ECL substrate	Thermo Fisher Scientific	34094
TEMED	Sisco Research Laboratories	52145

Hygromycin	Sigma-Aldrich	H0654
Ribopure RNA purification kit-Yeast	Thermo Fisher Scientific	AM1926
BCA Protein Assay kit	Thermo Fisher Scientific	23227
GMS Staining kit	ABcam	AB287884
Softwares		
RStudio v4.3.2	Posit	Not applicable
GraphPad Prism v9	GraphPad software	Not applicable
ImageJ		Not applicable
Other		
Glass beads	HiMedia	GRM2228
MATRIX thermoshaker	IKA	Not applicable
Spectrophotometer	Thermo Fisher Scientific	Not applicable
Proflex PCR systems	Thermo Fisher Scientific	Not applicable
MVX10 Stereo Microscope	OLYMPUS Scientific	Not applicable
Biosafety Cabinet	IGene Labserve	Not applicable
PVDF membrane	Milipore	IPVH00010
Mini Trans-Blot Cell Module	Bio-Rad	Not applicable
ChemiDoc™ MP analyzer	Bio-Rad	Not applicable
QuantStudio Real-Time PCR System	Thermo Fisher Scientific	Not applicable
Apotome widefield fluorescence microscope	Zeiss	Not applicable
Centrifuge 5425R	Eppendorf	Not applicable

1519